

## 1 **Structure of an ant-mymecophile-microbe community**

2 Elena K. Perry<sup>1</sup>, Stefanos Siozios<sup>2</sup>, Gregory D. D. Hurst<sup>2</sup> and Joseph Parker<sup>1\*</sup>

3 <sup>1</sup>*Division of Biology and Biological Engineering, California Institute of Technology, 1200 E*  
4 *California Boulevard, Pasadena, CA 91125, United States of America*

5 <sup>2</sup>*Institute of Infection, Veterinary and Ecological Sciences, University of Liverpool, Ic2 Liverpool*  
6 *Science Park, 146 Brownlow Hill, Liverpool, L3 5RF, United Kingdom*

7 \*corresponding author: [joep@caltech.edu](mailto:joep@caltech.edu)

8 **Abstract:** Superorganismal ant colonies play host to a menagerie of symbiotic arthropods,  
9 termed myrmecophiles, which exhibit varying degrees of social integration into colony life. Such  
10 systems permit examination of how animal community interactions influence microbial  
11 assemblages. Here, we present an ecologically and phylogenetically comprehensive  
12 characterization of an ant-mymecophile-microbe community in Southern California. Using 16S  
13 rRNA profiling, we find that microbiotas of the velvety tree ant (*Liometopum occidentale*) and its  
14 cohort of myrmecophiles are distinguished by species-specific characteristics but nevertheless  
15 bear signatures of their behavioral interactions. We found that the host ant microbiome was  
16 diverse at all taxonomic levels; that of a myrmecophilous cricket was moderately diverse, while  
17 microbiotas of three myrmecophilous rove beetles (Staphylinidae), which have convergently  
18 evolved symbiosis with *Liometopum*, were dominated by intracellular endosymbionts. Yet,  
19 despite these compositional differences, similarities between ant and myrmecophile microbiotas  
20 correlated with the nature and intimacy of their behavioral relationships. Physical interactions  
21 such as grooming and trophallaxis likely facilitate cross-species extracellular microbial sharing.  
22 Further, phylogenetic comparisons of microbiotas from myrmecophile rove beetles and  
23 outgroups revealed a lack of co-cladogenesis of beetles and intracellular endosymbionts, and  
24 limited evidence for convergence among the myrmecophiles' intracellular microbiotas.  
25 Comparative genomic analyses of the dominant *Rickettsia* endosymbiont of the most highly  
26 socially integrated myrmecophile imply possible functions unrelated to nutrient-provisioning in  
27 the host beetle's specialized lifestyle. Our findings indicate that myrmecophile microbiotas  
28 evolve largely independently of the constraints of deep evolutionary history, and that the  
29 transition to life inside colonies, including social interactions with hosts, plays a significant role  
30 in structuring bacterial assemblages of these symbiotic insects.

## 31 **Introduction**

32 Insects constitute the bulk of global animal biodiversity and form integral components of both  
33 terrestrial and freshwater ecosystems (Scudder, 2017). Although many factors have been  
34 proposed to underlie insect diversification (Grimaldi & Engel, 2005), studies in numerous taxa  
35 have revealed that partnerships with symbiotic bacteria have been key to facilitating the  
36 exploitation of novel habitats and trophic resources (Engel & Moran, 2013). Insect-associated  
37 microbes have variously been shown to enable host survival on recalcitrant food sources  
38 (Douglas, 1998; Moran, McCutcheon, & Nakabachi, 2008; Russell et al., 2009; Salem et al., 2017;  
39 Zientz, Dandekar, & Gross, 2004), to synthesize chemical defenses (Piel, 2002), to influence  
40 communication, mating behavior and reproduction (Engl & Kaltenpoth, 2018; Wada-Katsumata  
41 et al., 2015), and to confer protection against parasites (Kaltenpoth & Engl, 2014; Koch &  
42 Schmid-Hempel, 2011; Oliver, Russell, Moran, & Hunter, 2003). Yet, despite efforts to  
43 characterize the many adaptive (and non-adaptive) roles that symbiotic microbe communities  
44 play in insect biology, knowledge of the converse relationship—how host ecology shapes the  
45 assembly and composition of the microbiome—remains scarce.

46 Both comparative studies, as well as experiments involving a small number of model  
47 insect species, indicate that host microbiotas can be influenced by habitat (Park et al., 2019; Yun  
48 et al., 2014), diet (Colman, Toolson, & Takacs-Vesbach, 2012; Majumder et al., 2020; Mason et  
49 al., 2020; Renelies-Hamilton, Germer, Sillam-Dussès, Bodawatta, & Poulsen, 2021),  
50 developmental stage (Jennings, Korthauer, Hamilton, & Benoit, 2019; Yun et al., 2014), and  
51 evolutionary history (Brooks, Kohl, Brucker, Opstal, & Bordenstein, 2016; R. T. Jones, Sanchez,  
52 & Fierer, 2013). Such studies have typically focused either on a single insect taxon, or have  
53 treated multiple insect taxa as separate, non-interacting entities. Yet, many of the central roles  
54 that insects play within the biosphere involve their interactions with other animal species. Such  
55 relationships—from predator-prey interactions to parasitic and mutualistic symbioses—are  
56 pervasive, and typify the biologies of many speciose insect clades (Bologna & Pinto, 2001;  
57 Feener & Brown, 1997; Godfray, 1994; Hölldobler & Wilson, 1990; Kathirithamby, 2009; Kistner,  
58 1979, 1982; Kovarik & Caterino, 2005; Parker, 2016; Pierce et al., 2002; Stadler & Dixon, 2005).  
59 The nature of these interactions has in many cases evolved to become obligate, leading to  
60 extreme specialization of one insect species on a single or small number of partners (Beeren et  
61 al., 2021; Elmes, Barr, & Thomas, 1999; Hawkins, 1994; Komatsu, Maruyama, & Itino, 2009;  
62 López-Estrada, Sanmartín, Uribe, Abalde, & García-París, 2021; Maruyama & Parker, 2017;

63 Strand & Obrycki, 1996). How such interspecies dependencies shape the evolution and  
64 composition of insect microbiotas remains an open question.

65 In other animal clades including mammals, growing evidence indicates that, in addition  
66 to host diet and phylogeny (Amato et al., 2019; Groussin et al., 2017), direct social interactions  
67 both within and between species can influence host-associated microbial communities. In  
68 chimpanzees, seasonal increases in social interaction correlate with increased similarity of gut  
69 microbiota (Moeller et al., 2016). In baboons, patterns of gut microbiome similarity can be  
70 predicted from social networks based on grooming interactions (Tung et al., 2015). Studies in  
71 humans have likewise correlated close social relationships and cohabitation with greater  
72 similarity of gut or skin microbiota (Dill-McFarland et al., 2019; Song et al., 2013). Similarly, dog  
73 owners share more members of their skin microbiota with their own pets than with other dogs,  
74 indicating that contact-mediated microbial exchange can occur between species, strongly  
75 influencing microbial community structure (Song et al., 2013). These observations imply that the  
76 degree of behavioral intimacy between interacting individuals—either within social groups or  
77 between species—may be a key parameter shaping animal microbiotas.

78 Here, we ask how the evolution of social behavioral relationships between insect species  
79 impacts their symbiotic bacterial communities. To address this question, we exploit a novel  
80 system: an ant species that is targeted by a cohort of socially parasitic insects. Many ants play  
81 keystone roles in terrestrial ecosystems and engage in relationships with diverse other  
82 arthropods (Hölldobler & Wilson, 1990; Parker & Kronauer, 2021). One pervasive mode of  
83 interaction occurs within the ant colony itself—a sheltered microhabitat that houses a  
84 concentration of resources in the form of ant brood and harvested food. Although ruthlessly  
85 policed against intruders, colonies are vulnerable to exploitation by an array of specialized  
86 arthropods that have evolved ways to evade recognition and gain entry (Kistner, 1979, 1982;  
87 Parker, 2016). Such organisms, termed “myrmecophiles”, are often obligately dependent on a  
88 single host ant species (Beeren et al., 2021; Elmes et al., 1999; Komatsu et al., 2009; Maruyama  
89 & Parker, 2017). To infiltrate colonies, myrmecophiles commonly employ deceptive strategies  
90 that permit them to forge intimate relationships with their unknowing hosts. Social integration of  
91 myrmecophiles typically hinges on chemical and behavioral adaptations, including mimicry of  
92 host ant pheromones (cuticular hydrocarbons; CHCs) (Akino, 2002; Bagnères, Blomquist,  
93 Bagnères, & Lorenzi, 2010; Beeren et al., 2018; Beeren, Schulz, Hashim, & Witte, 2011; Lenoir  
94 et al., 2012; Maruyama, Akino, Hashim, & Komatsu, 2009; Meer & Wojcik, 1982; Parker, 2016),  
95 or the secretion of so-called “appeasement compounds” that attenuate ant aggression and

96 foster the myrmecophile's acceptance into the nest (Akre & Hill, 1973; Cammaerts, 1992;  
97 Hölldobler, 1967, 1970; Hölldobler & Kwapich, 2019; Jordan, 1913; Parker & Grimaldi, 2014;  
98 Stoeffler, Tolasch, & Steidle, 2011). Once integrated into colonies, myrmecophiles can engage  
99 in intimate physical interactions with hosts, including reciprocal grooming, phoresy, and mouth-  
100 to-mouth feeding (trophallaxis) (Akre & Hill, 1973; Hölldobler, 1971; Hölldobler & Wilson, 1990;  
101 Kistner, 1979, 1982; Leschen, 1991; Parker, 2016). The obligate nature and extreme closeness  
102 of some ant-myrmecophile relationships provides a paradigm to explore how interspecies  
103 relationships influence microbial community structure in both the host and symbiont insects.

104 Our model ant-myrmecophile network centers on the ecologically dominant native ant of  
105 Southern California: the velvety tree ant, *Liometopum occidentale* (Formicidae: Dolichoderinae)  
106 (**Fig. 1A**). *Liometopum* ants form huge colonies numbering over one million workers, and patrol  
107 sectors of low- to mid-elevation oak and pine forest floor that can span tens to hundreds of  
108 meters in diameter (Hoey-Chamberlain, Rust, & Klotz, 2013; Wang, Patel, Vu, & Nonacs, 2010).  
109 Colonies of this ant house a large menagerie of myrmecophiles with different socially parasitic  
110 lifestyles and integrating strategies. By virtue of their distinct behaviors, these species permit  
111 insight into how different modes of interspecies interaction can impact symbiotic microbial  
112 assemblages. Prominent within *Liometopum* colonies are multiple species of rove beetle  
113 (Staphylinidae) that are obligately associated with this ant, and for which detailed understanding  
114 of ethology and chemical ecology has been obtained (Danoff-Burg, 1996). Crucially, each rove  
115 beetle species has independently evolved to socially parasitize *Liometopum* colonies: the  
116 species all belong to the same rove beetle subfamily, Aleocharinae (Staphylinidae), but have  
117 evolved into myrmecophiles from phylogenetically distant free-living ancestors belonging to  
118 different taxonomic tribes. This property permits comparisons of microbiota between the  
119 convergent myrmecophiles and outgroup lineages, potentially illuminating how the evolution of  
120 behavioral symbioses shapes the microbiome.

121 In this study, we harness these attributes of the *Liometopum*-myrmecophile network to  
122 address how the social behaviors, evolutionary histories and microhabitats of interacting insect  
123 species contribute to structuring their symbiotic microbiotas. By extensive community sampling  
124 of core members of the myrmecophile network across colonies and localities, we have  
125 constructed a comprehensive, quantitative picture of the microbiome of an ant colony and its  
126 main social parasite symbionts. Incorporating knowledge of both myrmecophile behavior and  
127 microbiome data from outgroup relatives of key members of the myrmecophile network, we

128 present evidence that the intimacy of interspecies social relationships is a major determinant  
129 shaping the evolution of insect bacterial communities.

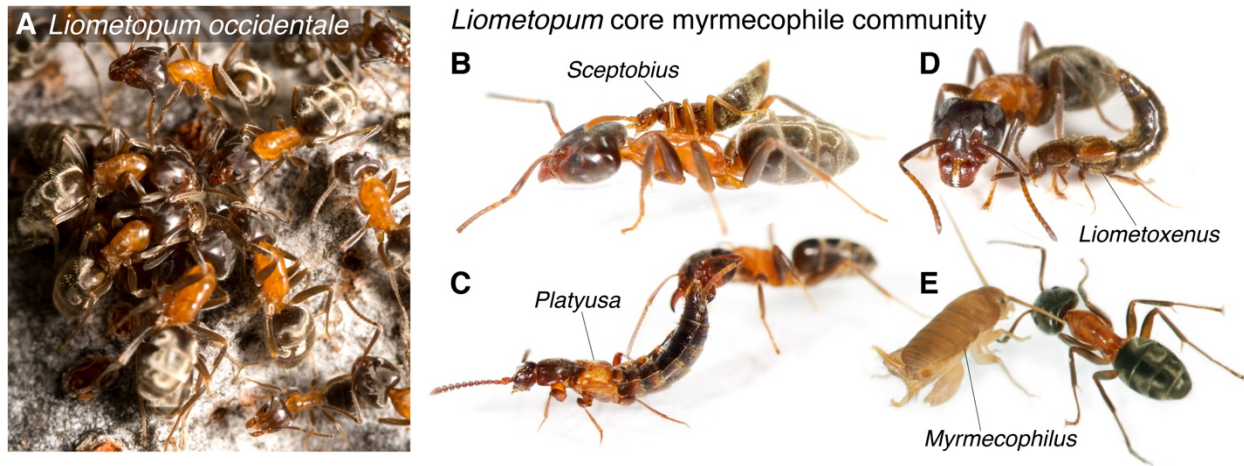


**Figure 1. The *Liometopum* myrmecophile community.** **A:** Workers of the velvety tree ant (*Liometopum occidentale*) foraging on a tree trunk. Credit: Kim Moore. **B:** *Sceptobius lativentris* rove beetle mounted on a *Liometopum* worker, performing grooming behavior. **C:** *Platyusa sonomae* rove beetle exuding appeasement secretion from abdominal gland to a *Liometopum* worker's mouthparts. **D:** *Liometoxenus newtonarum* rove beetle with *Liometopum* nearby. **E:** *Myrmecophilus* cf. *manni* cricket interacting with a *Liometopum* worker.

## 130 **Materials and Methods**

### 131 **Sample collection**

132 Specimens of *Liometopum*, *Sceptobius*, *Myrmecophilus*, *Platyusa*, and *Liometoxenus* were  
133 collected in Southern California in May and July, 2019 (see "Collection localities" below). The  
134 specimens were collected into sterile 50 mL conical tubes, with each species in separate tubes,  
135 and stored at 4°C until processing later the same day. For dissected samples, specimens were  
136 transferred to sterile 1.5 mL microcentrifuge tubes and washed by vortexing at high speed for  
137 10 s in 527  $\mu$ L of sterile TE buffer (10 mM Tris-HCl, 1 mM EDTA, pH 8) just prior to dissection;  
138 the TE buffer fractions were retained as "body wash" samples and stored at -80°C. Whole body  
139 specimens were washed in the same manner (except for *Pella*, *Lasius*, *Drusilla*, and *Lissagria*),  
140 transferred to fresh sterile microcentrifuge tubes, and stored at -80°C. *Sceptobius* and *Platyusa*  
141 were dissected to separate the head and the gut from the rest of the body, while for *Liometopum*  
142 only the gut was separated from the rest of the body. For *Sceptobius*, due their small body size,  
143 three individuals were pooled per dissected body part sample (single individuals were used in  
144 the case of whole body samples) to ensure sufficient DNA yields due to the small size of the  
145 beetles. The dissections were performed in sterile Petri dishes using forceps and dissecting

146 scissors that were sterilized in between samples with 10% bleach and flaming with ethanol.  
147 Dissected body parts were placed in fresh sterile 1.5 mL microcentrifuge tubes and immediately  
148 stored at -80°C until DNA extraction.

#### 149 **Collection localities**

150 Post Tree: USA, California, Altadena, Chaney Trail, 34.216293 -118.145922, 26 vii 2019, coll. E.  
151 Perry and J. Parker

152 First Tree: USA, California, Altadena, Chaney Trail, 34.216436 -118.148452, 26 vii 2019, coll. E.  
153 Perry and J. Parker

154 Rocks Tree: USA, California, Altadena, Chaney Trail, 34.217124 -118.154182, 26 vii 2019, coll.  
155 E. Perry and J. Parker

156 Sleepy Tree: USA, California, Altadena, Chaney Trail, 34.217456 -118.154426, 26 vii 2019, coll.  
157 E. Perry and J. Parker

158 Mile High Tree: USA, California, Altadena, Rubio Canyon Trail, 34.2053886, -118.1176927, 22 v  
159 2019, coll. E. Perry and J. Parker

#### 160 **DNA extraction and sequencing**

161 DNA extractions were performed in batches of 11 samples, with one blank extraction per batch.  
162 To minimize the possibility of confounding batch effects with true differences between samples,  
163 each batch consisted of a random assortment of different sample types. To maximize bacterial  
164 DNA yield, the extractions were performed using a multistage protocol that involved grinding  
165 samples in liquid nitrogen, bead beating, and several rounds of phenol-chloroform extraction as  
166 described below.

167 Prior to starting extractions, 0.1 mm glass beads were sterilized by baking at 280°C for 4  
168 hours. Working in a biological safety cabinet to maintain sterility, approximately 100 µL of beads  
169 were then transferred into each sample tube using a spatula sterilized with 50% bleach. After  
170 adding the beads, the samples (except for body wash samples) were ground to a fine powder in  
171 liquid nitrogen using blunt metal forceps that were sterilized in between samples with 50%  
172 bleach and flaming with ethanol. 527 µL of TE buffer was added to each tube immediately after  
173 grinding, except for body wash samples, which already consisted of the same volume of TE  
174 buffer; the latter were thawed on ice. Subsequently, 60 µL of 10% sodium dodecyl sulfate (SDS),  
175 7.5 µL of proteinase K (20 mg/mL), and 6 µL of lysozyme (100 mg/mL) were added to each

176 sample. The tubes were subjected to bead beating in a Disruptor Genie (Scientific Industries,  
177 Inc.) for 1 min at 4°C, and then incubated overnight at 37°C with shaking at 250 rpm.

178 The following day, 100 µL of 5 M NaCl was added and mixed thoroughly, followed by the  
179 addition of 80 µL of CTAB/NaCl solution (10% cetyltrimethylammonium bromide, 0.7 M NaCl)  
180 preheated to 65°C. The samples were incubated at 65°C for 10 min with periodic mixing by  
181 inversion. Next, 650 µL of 25:24:1 phenol/chloroform/isoamyl alcohol (pH 8) was added and  
182 mixed thoroughly by inversion, and the samples were spun at 13,000 rpm for 5 min in a  
183 microcentrifuge. The aqueous supernatant was transferred to a fresh 1.5 mL microcentrifuge  
184 tube and the extraction was repeated with 700 µL of 24:1 chloroform/isoamyl alcohol. Finally,  
185 the aqueous layer was extracted a third time with 500 µL of 24:1 chloroform/isoamyl alcohol. In  
186 addition, 650 µL of fresh TE buffer was added to the first round of phenol/chloroform/isoamyl  
187 alcohol tubes and the entire three-step extraction process was repeated, such that each organic  
188 fraction was extracted twice. Both aqueous fractions were then combined for each sample in a  
189 1.5 mL DNA LoBind microcentrifuge tube (Eppendorf). DNA was precipitated overnight at -20°C  
190 with 0.6 vol isopropanol and 1 µL GenElute linear polyacrylamide (MilliporeSigma). Following  
191 precipitation, the DNA was pelleted by centrifuging at 13,000 rpm for 30 min at 4°C. The pellets  
192 were washed twice with 70% ethanol, then air dried and resuspended in 25 µL of 10 mM Tris  
193 buffer (pH 8). Resuspension was allowed to proceed overnight at 4°C prior to quantification of  
194 DNA yield using the Qubit dsDNA HS assay kit (ThermoFisher Scientific).

195 16S V4 amplification and Illumina library preparation were performed by Laragen, Inc.,  
196 following the protocol recommended by the Earth Microbiome Project (Ul-Hasan et al., 2019).  
197 For approximately half of the samples (not limited to particular sample types), PCR amplification  
198 initially failed. Most of these samples ultimately yielded a detectable gel electrophoresis band  
199 upon the inclusion of 100 mg/mL bovine serum albumin in the reaction, or after further sample  
200 purification using the DNeasy PowerClean CleanUp kit (QIAGEN) and/or use of the KAPA3G  
201 Plant PCR kit (Roche) instead of Platinum Hot Start PCR Master Mix (ThermoFisher Scientific).  
202 The full list of sample treatments (excluding blank samples) is provided in **Table S1**. Amplified  
203 samples were sequenced on the Illumina MiSeq platform using the MiSeq v2 300 cycles kit  
204 (Illumina).

## 205 **16S rRNA gene amplicon sequence processing and curation**

206 MiSeq data were processed using the dada2 R package (version 1.14.1) (Callahan et al., 2016)  
207 to perform quality control (trimming and filtering) on sequences, infer exact amplicon sequence

208 variants (ASVs), remove chimeras, and assign taxonomy to ASVs. The sequences were  
209 processed according to the dada2 pipeline recommendations  
210 (<https://benjjneb.github.io/dada2/tutorial.html>), but with a maximum of only one expected error  
211 allowed per read, and the truncation length set to 140. Taxonomy was assigned in dada2 using  
212 the SILVA reference database (version 132) (Quast et al., 2013).

213 ASVs identified as chloroplasts, mitochondria, or eukaryotic were removed from the data  
214 set using QIIME 2 (version 2020.2) (Bolyen et al., 2019). Additional putative contaminant  
215 sequences were identified and removed using the decontam R package (version 1.6.0) (Davis,  
216 Proctor, Holmes, Relman, & Callahan, 2018) in conjunction with phyloseq (version 1.30.0)  
217 (McMurdie & Holmes, 2013). ASVs were considered likely contaminants if they were identified  
218 as such both by frequency in negative controls vs. true samples and by prevalence across  
219 negative controls vs. true samples (using the default  $p$ -value threshold of 0.1). The blank DNA  
220 extractions served as the negative controls. For the frequency metric, the number of reads from  
221 each sample was used as a proxy for DNA concentration.

222 Following the removal of putative contaminants, all further sequence processing was  
223 performed in QIIME 2. First, the reference sequences were aligned and a phylogenetic tree was  
224 generated using the command “align-to-tree-mafft-fasttree.” Then, samples were rarefied to  
225 1000 reads; five samples were discarded due to falling below this threshold. Alpha diversity  
226 metrics (Simpson index and chao1 estimate) were calculated, and beta diversity distance  
227 matrices (based on Bray-Curtis dissimilarity, Jaccard distance, and weighted and unweighted  
228 UniFrac distances) were generated. Inspection of principal coordinates analysis plots generated  
229 in QIIME 2 for the different distance metrics revealed no obvious clustering of samples based on  
230 differential treatment during sample cleanup or PCR amplification. For insect body part and  
231 whole body samples, beta diversity analyses were performed both before and after filtering out  
232 putative intracellular endosymbiont ASVs, while for body wash samples, the analyses were  
233 performed before and after filtering out all ASVs that appeared in any nest sample. Finally, after  
234 filtering out ASVs with fewer than 10 reads total across all samples to reduce the number of  
235 zeroes in the feature table, ASVs that were differentially abundant across *Liometopum*,  
236 *Sceptrobius*, *Myrmecophilus*, and *Platyusa* samples (excluding putative intracellular  
237 endosymbionts and body wash samples) were identified using the QIIME 2 DS-FDR (discrete  
238 false discovery rate control) plugin with Kruskal-Wallis tests (Jiang et al., 2017).



## 239 **Genome sequencing, assembly, and annotation**

240 For Illumina sequencing we used a single *Sceptobius lativentris* female (USA: California, Altadena,  
241 Eaton Canyon Falls Trail, 34°11'38.1"N 118°06'11.8"W vi.2017, coll. J. Parker). Genomic DNA  
242 was isolated via phenol/chloroform method, and integrity was assessed with a Bioanalyzer. An  
243 Illumina paired-end library (150bp) was prepared using the Illumina TruSeq DNA kit and  
244 sequenced on the Illumina HiSeq X platform by Iridian Genomes/J. Parker and collaborators.  
245 Reads were deposited on NCBI's Sequence Read Archive (accession: SRR5909496). For long  
246 reads, total genomic DNA was extracted from 20 *Sceptobius* males and sequenced on an Oxford  
247 Nanopore minION flow cell at the Millard and Muriel Jacobs Genetics and Genomics Laboratory  
248 at Caltech. An initial assembly of the Illumina reads from the SRR5909496 library was assembled  
249 *de novo* using megahit v1.2.9 (D. Li, Liu, Luo, Sadakane, & Lam, 2015) and the contigs were  
250 binned using Metabat2 (Kang et al., 2019) based on tetranucleotide frequencies. A *Rickettsia* like  
251 bin was identified using CheckM v1.0.13 (Parks, Imelfort, Skennerton, Hugenholtz, & Tyson,  
252 2015) and was used as a reference to map both short and long reads using minimap2 (H. Li,  
253 2018). The *Rickettsia* like reads were extracted with samtools v1.9 (H. Li et al., 2009) and a hybrid  
254 assembly of Nanopore and Illumina reads was performed using the Unicycler pipeline v0.4.8  
255 under the normal mode (Wick, Judd, Gorrie, & Holt, 2017). The raw reads (long and short) were  
256 mapped back to the assembly and the assembly was visually inspected for misassemblies.  
257 Genome annotation was performed with prokka v1.14.0 (Seemann, 2014) and Pfam domains  
258 were predicted with InterProScan v86.0 (P. Jones et al., 2014). Genomic contigs as well as the  
259 complete annotated genome and annotation is provided in **Files S1, S2** and **Table S5**.

## 260 **Phylogenomic analysis**

261 The phylogenetic position of the *Rickettsia* endosymbiont of *Sceptobius lativentris* was estimated  
262 in relation to 86 publicly available genomes from all major *Rickettsia* groups based on the  
263 concatenated analysis of 267 single copy core proteins determined using OrthoFinder v2.3.11  
264 (Emms & Kelly, 2019). Phylogenetic relationships were inferred using maximum likelihood as  
265 implemented in IQ-TREE 2.0.3 (Minh et al., 2020) under the JTT+F+R5 model which was selected  
266 using ModelFinder (Kalyaanamoorthy, Minh, Wong, Haeseler, & Jermini, 2017). The robustness  
267 of the tree was finally assessed based on 1000 ultrafast bootstrap replicates (Hoang, Chernomor,  
268 Haeseler, Minh, & Vinh, 2017). The phylogenetic tree was visualized and annotated using iTOL  
269 (Letunic & Bork, 2007).

## 270 **Comparative genomic and metabolic analysis**

271 A comparative genomic analysis across members of the Transitional group of *Rickettsia* was  
272 performed using anvi'o package v7 (Eren et al., 2021). The following parameters were used to  
273 create the pangenome of the transitional group: "--use-ncbi-blast --mcl-inflation 1.5". The  
274 metabolic potential of RiSlat genome was estimated using the "anvi-estimate-metabolism"  
275 program from anvi'o package by computing the completion ratio of the predicted KEGG  
276 functional categories and compared to the other members of the transitional group. Heatmaps  
277 were prepared using the R package pheatmap (Kolde & Kolde, 2015). We computed the fraction  
278 of interrupted genes (genes which length was shorter than 80% of their best hit in the Swiss-  
279 Prot database) using the ideel method (<https://github.com/mw55309/ideel>). Finally, repeat  
280 density (repeats  $\geq$  1500 bp and at least 95% identity) in RiSlat genome and the synteny between  
281 RiSlat genome and complete reference genomes from the transitional group of *Rickettsia* was  
282 computed and visualized using MUMmer v3 (Kurtz et al., 2004).

## 283 **Data analysis and statistics**

284 Non-metric multidimensional scaling (NMDS) ordinations were generated using the R package  
285 vegan (version 2.5-6) (Oksanen et al., 2015). Permutational multivariate analysis of variance  
286 (PERMANOVA) was performed on distance matrices using the "adonis" function in vegan with  
287 999 permutations. Distributions of distances between different sample types were compared in  
288 R either using the Wilcoxon test followed by the Benjamini-Hochberg method to control the false  
289 discovery rate for multiple comparisons, or using the Kruskal-Wallis test followed by Dunn's test  
290 for pairwise comparisons. Dunn's test was performed using the function "dunnTest" from the  
291 package FSA (Ogle, Wheeler, & Dinno, 2020). Complete information on the statistical tests used  
292 in each figure is provided in **Table S2**. Plots in **Figs. 2-4** and **Figs. S1-S3** were generated in R  
293 with the package ggplot2 (version 3.3.1) (Wickham, 2011) except that the package pheatmap  
294 (Kolde & Kolde, 2015) was used to generate the heatmap in **Fig. 3C**, and the package bipartite  
295 (version 2.15) (Dormann, Gruber, & Fründ, 2008) was used to generate the bipartite network plot  
296 in **Fig. 4B**.

## 297 **Results**

### 298 **The *Liometopum*-myrmecophile community**

299 Our study sites are located in the foothills of the San Gabriel Mountains within Angeles National  
300 Forest, LA County, California, where *Liometopum occidentale* is the predominant ant species.  
301 We have found that colonies of this ant play host to a “core” community of four obligate  
302 myrmecophiles, which occur in and around most, if not all nests, and exhibit distinct behavioral  
303 interactions with host workers. Three members of the core community belong to the  
304 hyperdiverse rove beetle subfamily Aleocharinae (Coleoptera: Staphylinidae)—a clade of  
305 ~17,000 species in which numerous lineages have evolved myrmecophilous lifestyles (Kistner,  
306 1979; Maruyama & Parker, 2017; Parker, 2016; Seevers, 1965; Yamamoto, Maruyama, & Parker,  
307 2016). One of these species, *Sceptobius lativentris* (Aleocharinae: Sceptobiini) ranks among the  
308 most socially integrated myrmecophiles known. *Sceptobius* beetles live in close physical  
309 intimacy with host ants, climbing onto workers’ bodies where they spend up to 80% of their  
310 adult lives (**Fig. 1B; Video S1**). Attaching to workers enables the beetle to groom the ant with its  
311 legs—an adaptive behavior that functions to transfer the ant’s CHCs onto the beetle’s own body.  
312 Ant grooming permits *Sceptobius* to achieve identical chemical resemblance to its host and gain  
313 social acceptance, reflected in the presence of beetles throughout the nest, including the brood  
314 galleries. *Sceptobius* is believed to feed on ant brood as well as via trophallaxis with workers,  
315 and may also perform “strigilation”—grazing on material attached to worker body surfaces  
316 (Danoff-Burg, 1996). The beetles are unable to survive for longer than ~24 hours without direct,  
317 physical interactions with *Liometopum* workers (Danoff-Burg, 1996). *Sceptobius* thus embodies  
318 the phenotypic extreme of socially complex symbiotic lifestyles, and is the most tightly  
319 associated of the core *Liometopum* myrmecophiles.

320 The second myrmecophile, the aleocharine *Platyusa sonomae* (Aleocharinae:  
321 Lomechusini), is behaviorally distinct to *Sceptobius*: it occurs in the vicinity of colonies and along  
322 ant foraging trails but appears never to penetrate inside the nest. *Platyusa* interacts physically  
323 but transiently with ants: the beetles appease and pacify aggressive workers with attractive  
324 secretions from an abdominal gland (**Fig. 1C**). Additionally, physical interactions occur through  
325 direct predation on worker ants. Unlike *Sceptobius*, *Platyusa* can be cultured independently of  
326 its host ant in the laboratory and fed alternative diets. The third aleocharine, *Liometoxenus*  
327 *newtonarum* (Aleocharinae: Oxypodini) is found predominantly at the mouths of nests where ant  
328 density is high, but we have not observed this species deeper in the colony. *Liometoxenus*

329 intermingles with ant workers (**Fig. 1D**), but does not groom them; instead, *Liometoxenus*  
330 produces a volatile, ester-rich cocktail from an abdominal gland that acts at a distance,  
331 ‘intoxicating’ ants and impeding their locomotion. Like *Platyusa*, *Liometoxenus* also predates on  
332 worker ants. Unlike the other core myrmecophiles which are found commonly year-round,  
333 *Liometoxenus* adults appear only during spring, and are somewhat rarer. The final core  
334 myrmecophile is the ant cricket, *Myrmecophilus cf. manni* (Orthoptera: Myrmecophilidae).  
335 Behavioral studies of this and other *Myrmecophilus* species, as well as our own observations,  
336 have shown that the crickets interact closely with ants (**Fig. 1E**), feeding via both trophallaxis  
337 with workers and also via opportunistic strigilation, wherein the cricket rapidly approaches the  
338 ant and briefly grazes its body surface before retreating (Hebard, 1920; Henderson & Akre, 1986;  
339 Morton, 1900). These actions parallel some behaviors of *Sceptobius*. However, *Myrmecophilus*  
340 is not phoretic upon *Liometopum* workers, does not groom them, and based on our observations,  
341 does not access the internal parts of colonies but instead inhabits nest entrances and trails.

342 The distinct trophic and physical interactions between the four myrmecophiles and their  
343 shared *Liometopum* host ant motivated us to ask how their contrasting lifestyles are reflected in  
344 their microbial symbionts. We generated bacterial 16S rRNA metabarcoding libraries from  
345 *Liometopum* workers and each of the core myrmecophile species, sampling specimens from five  
346 ant colonies in two field sites in the Angeles National Forest (see **Materials and Methods**). For  
347 all species, we sequenced whole insect bodies, as well as microbes washed from the body  
348 surface. Further, given the myrmecophiles’ diverse modes of social interaction and feeding  
349 behavior, we also sequenced specific microbial communities from the gut and body of  
350 *Liometopum* host workers, and from the gut, head and body of the myrmecophiles *Sceptobius*  
351 and *Platyusa*. The latter two species display the most divergent trophic behaviors, and in  
352 behavioral terms represent the most and least extreme degrees of social integration into the host  
353 colony. Since each of the rove beetles has convergently evolved to target *Liometopum*, we  
354 additionally asked to what extent the microbial communities of *Sceptobius* and *Platyusa* are  
355 influenced by their evolutionary histories. To do so, we sequenced whole-body microbiota from  
356 free-living outgroups of both species: for *Sceptobius*, we obtained the North American  
357 aleocharine *Lissagria laeviuscula* (tribe Falagriini: the sister tribe of Sceptobiini, or from which  
358 Sceptobiini is a derived lineage; Danoff-Burg, 1994, 2002; Maruyama & Parker, 2017), while for  
359 *Platyusa*, we obtained the European aleocharine *Drusilla canaliculata* (tribe Lomechusini). We  
360 also obtained specimens of the European aleocharine *Pella cognata* (tribe Lomechusini)—a  
361 myrmecophilous close relative of *Platyusa*, which is associated with a different host ant, the

362 formicine *Lasius fuliginosus* (the microbiome of which we also sequenced). In total, we  
363 sequenced 230 libraries from the host ant, the four core myrmecophiles, environmental nest  
364 material from each sampled colony, blank (control) samples, as well as replicate libraries from  
365 each outgroup species and host ant.

### 366 **Microbiome of the velvety tree ant**

367 We determined the taxonomic composition and alpha diversity of each species' microbiota by  
368 quantifying bacterial 16S rRNA amplified sequence variants (ASVs)—a proxy for species (**Fig.**  
369 **2A**). Of all species surveyed, the host ant, *Liometopum occidentale*, possessed the most diverse  
370 microbiota by two different metrics: the Simpson index, which is influenced by both species  
371 richness and evenness within each sample, and the chao1 estimate of total species richness  
372 (**Fig. 2B, C**). In addition to alpha diversity at the ASV level, the *Liometopum* microbiota was also  
373 the most diverse at the phylum level, encompassing Proteobacteria, Firmicutes, Actinobacteria,  
374 Bacteroides, Acidobacteria, Planctomycetes, and Verrucomicrobia—each comprising at least 1%  
375 of the 16S reads from pooled ant body or gut samples (**Fig. 2A**). Taxonomic composition at the  
376 phylum level was qualitatively similar across pooled *Liometopum* wash, body and gut samples,  
377 but generally distinct from the nest samples. For example, the majority of the latter contained a  
378 high proportion of reads from a single ASV classified as *Klebsiella*, which was nearly absent from  
379 the *Liometopum* samples, while many *Liometopum* samples had high proportions of Firmicutes,  
380 which were nearly absent from nest samples (**Fig. 2A, Fig. S1**). These distinctions suggest that  
381 *Liometopum*'s microbiota is typically distinct from its own nest material, and that physiological  
382 characteristics of *Liometopum* likely influence the assembly of its microbiota.

383 Despite coarse similarity among microbiota samples at the phylum level, however,  
384 *Liometopum* guts did not possess a distinctive “core” microbiota across samples, defined here  
385 as the set of ASVs present in at least 90% of the samples of a given species and body part (see  
386 **Table S1** for ASV abundances, both per sample and means per sample type). Across  
387 *Liometopum* body samples, only ASV6 (*Sphingomonas*) was highly prevalent, albeit at a low  
388 relative abundance (median of 0.55%). This same ASV was also present in several other species  
389 at a similar abundance (**Table S1**), and we cannot rule out this it is a contaminant (Salter et al.,  
390 2014). We also found no evidence for obligate, intracellular endosymbionts among the  
391 *Liometopum* microbiota. Such endosymbionts are typically known from ant species that utilize  
392 more specialized food sources than the generalized, omnivorous/scavenger diet of *L.*  
393 *occidentale* (Feldhaar et al., 2007; Gil et al., 2003).

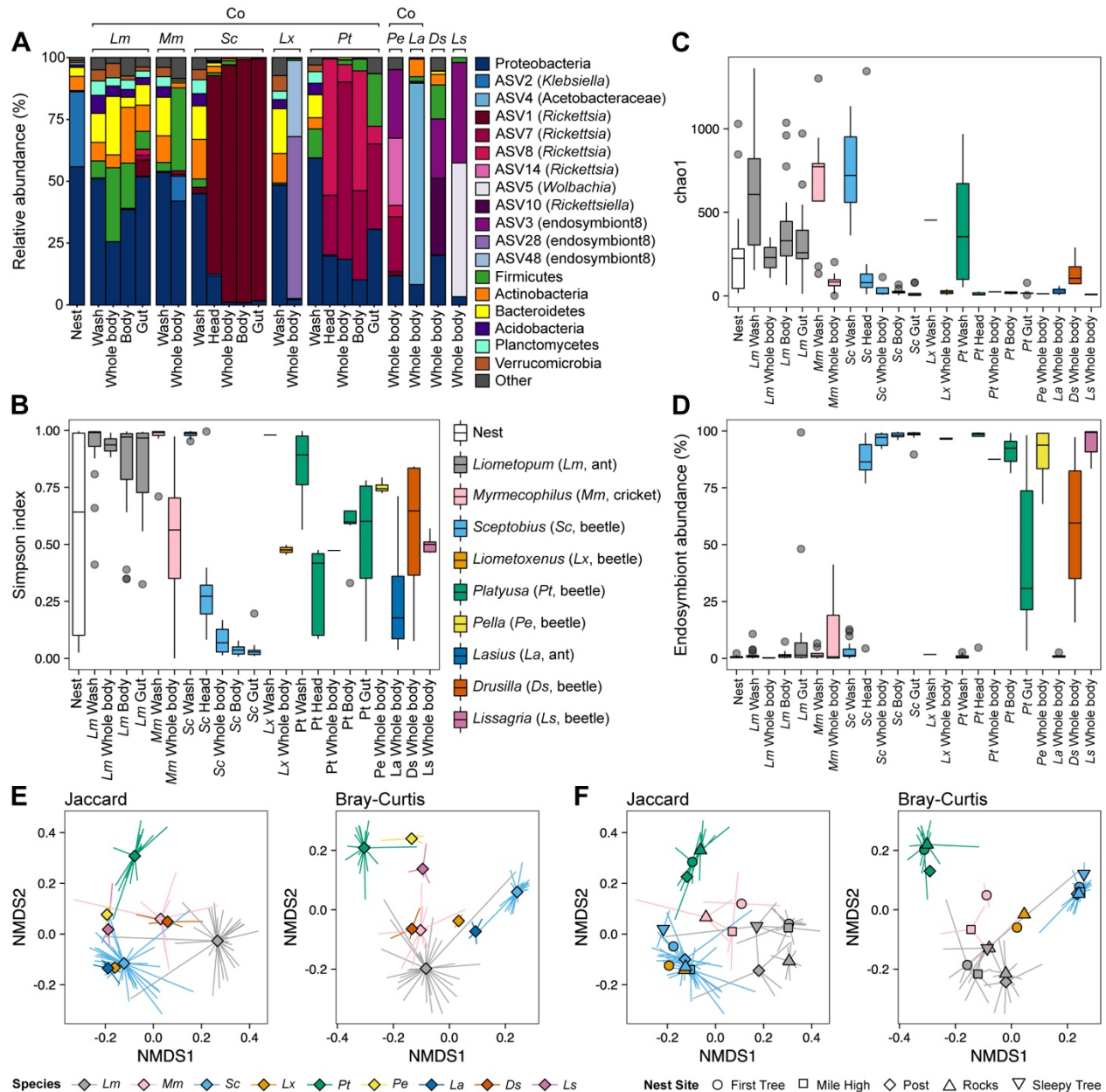


**Figure 2. Microbial diversity of *Liometopum* and core myrmecophiles.** **A:** Bar plots showing relative abundance of different bacterial taxa in the studied species. Samples belonging to the same insect species and sample type were combined additively. Lm = *Liometopum* (ant), Mm = *Myrmecophilus* (cricket), Sc = *Sceptobius* (beetle), Lx = *Liometoxenus* (beetle), Pt = *Platyusa* (beetle), Pe = *Pella* (beetle), La = *Lasius* (ant), Ds = *Drusilla* (beetle), Ls = *Lissaggria* (beetle). “Co” indicates species that cohabitate. Taxa bar plots for individual samples are provided in **Fig. S1**. **B-D:** Distributions of alpha diversity metrics for each sample type, as quantified by the Simpson index (**B**), chao1 species richness estimate (**C**), and relative abundance of putative endosymbionts (**D**). The color legend in panel B also applies to panels C and D. **E-F:** NMDS ordination of the insect samples (not including wash samples) based on either Jaccard distance (unweighted by abundance) or Bray-Curtis dissimilarity (weighted by abundance). Diamonds (**E**) or other shapes (**F**) mark the centroids of each species or sample group, while line segments connect the centroids to the individual data points. Centroids and line segments are colored by the species of origin in both E and F, and in F the marker shape for the centroid of each group denotes the nest site where the samples were collected. Not all samples from E are shown in F, as site information was only available for *Liometopum* and its associated myrmecophiles.

## 394 **Species-specific characteristics of myrmecophile microbiotas**

395 With the exception of body wash samples, microbial alpha diversities of the four core  
396 myrmecophiles were all markedly lower than that of the host ant. The cricket, *Myrmecophilus*,  
397 harbored the greatest diversity at both the ASV and phylum levels, with large proportions of both  
398 Proteobacteria and Firmicutes (42% and 34% respectively across pooled samples; **Fig. 2A, Fig.**  
399 **S1**). Median Simpson index and chao1 estimates from whole body samples were 0.56 and 83,  
400 respectively (**Fig. 2B, C**). Like its host ant, however, *Myrmecophilus* also did not possess a  
401 distinctive, core microbiota at the ASV level (**Table S1**). *Sceptobius* exhibited the least diverse  
402 microbiota, with Simpson index values of 0.03-0.27, depending on the body part, and  
403 correspondingly low chao1 estimates (**Fig. 2B, C**). The two remaining rove beetles, *Platyusa* and  
404 *Liometoxenus*, both exhibited intermediate Simpson index values of 0.48 (**Fig. 2B**). However, the  
405 chao1 species richness estimates for *Platyusa* and *Liometoxenus* were both low (16.5 and 22,  
406 respectively; excluding wash samples), indicating that these species' higher Simpson index  
407 values likely reflected greater evenness of the microbial communities relative to *Sceptobius*  
408 rather than greater species richness.

409 The most striking feature of the microbiotas of all three staphylinids was the high  
410 proportions of reads from putative intracellular endosymbionts (**Fig. 2D, Fig. S1**). For example,  
411 >95% of 16s reads from *Sceptobius* bodies and guts belonged to a single variant of the  
412 intracellular Proteobacteria genus *Rickettsia*. This variant, ASV1, also accounted for 80% of  
413 reads from *Sceptobius* heads, indicating its likely presence throughout the body (**Fig. 2A; Table**  
414 **S1**). Similarly, *Rickettsia* species dominated the *Platyusa* microbiota, with three variants, ASV7,  
415 ASV8, and ASV40, that were differentially abundant across different body parts (**Fig. 2A, Fig. S1;**  
416 **Table S1**). ASV8 was more abundant in the head (median relative abundance of 66.8%) and  
417 body (43.1%) compared to the gut (2.9%), while ASV40 was most prevalent and abundant in  
418 *Platyusa* body samples (median relative abundance of 7.2%), but absent from head samples.  
419 ASV7 was generally present in similar proportions in all types of sequenced body parts (median  
420 relative abundance of 28-44%) and was also present at a comparable frequency in one  
421 undissected *Platyusa* whole body (**Fig. 2A, Fig. S1; Table S1**). Although *Liometoxenus* lacked  
422 *Rickettsia*, its microbiota was nevertheless dominated by two variants of a putative  
423 endosymbiont named "endosymbiont8" in the SILVA reference database (Quast et al., 2013).  
424 These ASVs, 28 and 48, belong to the Enterobacteriaceae family with 91-92% BLAST similarity  
425 to *Providencia* (the closest genus match), and collectively account for 95% of reads from this

426 beetle species (**Fig. 2A, D; Table S1**). Beyond these dominant endosymbionts, the rove beetles  
427 possessed few other core microbial taxa: the aforementioned *Sphingomonas* (ASV6) was the  
428 only other consistently recovered non-intracellular bacterium in *Sceptobius*, specifically in the  
429 body and gut, and was present at low levels (0.2 and 0.5% median relative abundance  
430 respectively), while *Platyusa* did not possess any core ASVs other than ASV8 in either the head,  
431 body, or gut (**Table S1**). As for *Liometoxenus*, two *Arhodomonas* taxa, ASV6 and ASV39 were  
432 the only other two sequence variants present in both samples, at median relative abundances of  
433 1.7 and 0.25% respectively (**Table S1**).

#### 434 **Both species and colony identity impact host ant and myrmecophile microbiotas**

435 NMDS ordinations based on both Jaccard distances and Bray-Curtis dissimilarities revealed that  
436 samples tended to cluster by species, with some overlap (**Fig. 2E**). PERMANOVA analysis  
437 revealed a statistically significant effect of species ( $p = 0.001$ ; **Table S2**), confirming that the ant  
438 and its myrmecophiles possess distinguishable microbiotas. Given the relatively low shared  
439 diversity of microbial taxa across individuals within each insect species, however, we asked  
440 whether microbiotas were also potentially shaped by colony-level factors. Differences between  
441 source colonies may derive from ‘background’ environmental microbes that are not necessarily  
442 symbiotic. Alternatively, there may be colony-level differences in symbiotic microbiota, reflecting  
443 differential acquisition of microbes that are associated with host insect physiology. To distinguish  
444 between these possibilities, we performed NMDS ordination (**Fig. S2A**) and PERMANOVA on  
445 samples of collected nest material to determine whether background environmental microbes  
446 differed between colonies. For both Jaccard distance and Bray-Curtis dissimilarity,  
447 PERMANOVA revealed a statistically significant effect of nest site ( $p < 0.05$ ; **Table S2**), with  $R^2$   
448 ranging from 0.34 (Jaccard distance) to 0.42 (Bray-Curtis dissimilarity), reflected in moderate  
449 clustering in the ordination plots (**Fig. S2A**), confirming that environmental microbial communities  
450 indeed differed between colonies.

451 Before comparing insect samples from the different colonies, we verified whether the  
452 washes had effectively decreased reads from bacteria present in the nest environment, which  
453 we postulated would represent primarily transient, low-abundance members of the background  
454 microbiota rather than stably associated symbionts. Indeed, by both Jaccard distance and Bray-  
455 Curtis dissimilarity, wash samples were significantly more similar than insect body part samples  
456 to nest material samples (**Fig. S2B**). With the latter metric, there was also a long tail of samples



457 with relatively low dissimilarity between insect body parts and nest material, possibly because  
458 unlike Jaccard distance, Bray-Curtis dissimilarity is weighted by abundance and therefore less  
459 sensitive to low-abundance community members (Birtel, Walser, Pichon, Bürgmann, & Matthews,  
460 2015). Nevertheless, these results suggest that the washes successfully removed at least some  
461 environmentally derived bacteria. PERMANOVA analysis indicated that even after removing  
462 wash samples from the dataset, colony identity still had a significant effect ( $p = 0.001$ ; **Table S2**)  
463 on the microbiota associated with the ants and myrmecophiles, based on Jaccard distances,  
464 although insect species explained a larger proportion of variation than nest site. These trends  
465 can be seen in the NMDS ordination of samples grouped by either insect species (**Fig. 2E**) or  
466 nest site (**Fig. 2F**). The statistically significant effect of colony identity was primarily driven by  
467 body samples, as PERMANOVA did not reveal a significant effect of location when the analysis  
468 was restricted to either gut or head samples. The PERMANOVA analysis revealed that the  
469 interaction between nest site and insect species was statistically significant ( $p = 0.008$ ; **Fig. 2F**;  
470 **Table S2**), suggesting that inter-colony differences in the insect microbiotas were not driven by  
471 the same sets of microbes across the different species. These data uncover colony-to-colony  
472 variation in the symbiotic microbiota associated with each insect species—variation that is  
473 separate from background environmental microbiota present in nest material.

#### 474 **Social interaction strength correlates with microbial sharing**

475 Having established the relative contributions of colony differences and species-specific factors  
476 on microbiome structure, we asked to what extent social and trophic interactions with ants leave  
477 signatures in the core myrmecophile species' microbiota. *A priori*, we hypothesized that  
478 *Sceptradius* and possibly *Myrmecophilus* may possess microbial communities most similar to  
479 that of the host ant due to their close physical interactions with workers. To test this hypothesis,  
480 we first filtered out sequences from putative intracellular endosymbionts in order to highlight the  
481 fraction of the microbiota most likely to be horizontally transferred during insect behavioral  
482 interactions. We also removed *Liometoxenus* from this analysis because only one sample from  
483 this rare species still met the minimum threshold of 1000 reads after removing the putative  
484 endosymbiont sequences. We then compared the distributions of pairwise distances and  
485 dissimilarity metrics calculated for each myrmecophile species with respect to the ant host.  
486 Samples were compared within nest sites, due to the aforementioned effect of colony identity  
487 on microbial community composition (**Fig. 2F**; **Table S2**).

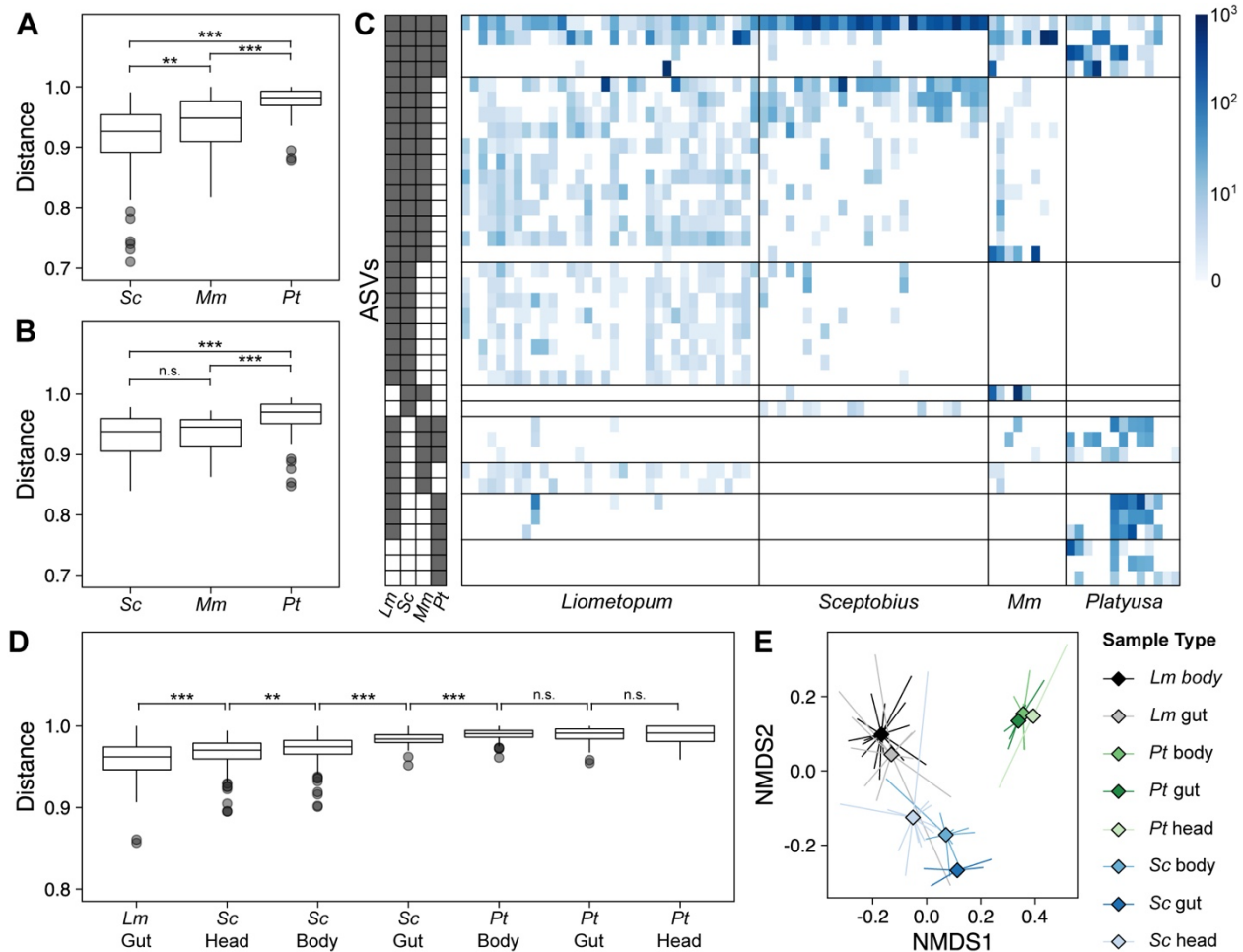


**Figure 3. Social interactions explain microbial sharing between ants and myrmecophiles.** **A:** Jaccard pairwise distances for *Sceptobius* (Sc), *Platyusa* (Pt), and *Myrmecophilus* (Mm) versus *Liometopum*, within nest sites, without endosymbionts. All sample types except wash samples (i.e. whole body samples in addition to dissected body parts where applicable) were included for each species. **B:** Jaccard pairwise distances for body washes of *Sceptobius* (Scep), *Platyusa* (Plat), and *Myrmecophilus* (Cric) versus *Liometopum*, within nest sites, after removing all ASVs that appeared in any Nest sample. **C:** Visualization of ASVs that were differentially abundant across ant, *Sceptobius*, cricket, and *Platyusa* samples, as determined by Kruskal-Wallis tests using the DS-FDR method to control the false discovery rate to 0.1. Left: Visualization of the presence (gray)/absence (white) of each ASV in samples pooled by insect species. Each row represents an ASV and the columns from left to right represent ant, *Sceptobius*, cricket, and *Platyusa* respectively. Right: Heatmap showing the normalized read counts for each ASV in each sample. Each row represents an ASV (same order as on the left), each column represents an individual sample, and the heatmap cells are colored by read count. See **Table S3** for the ASV identities and statistical values. **D:** Jaccard pairwise distances between different myrmecophile body parts and ant bodies, without endosymbionts. **E:** NMDS of Jaccard pairwise distances for *Sceptobius* (Sc), *Platyusa* (Pt), and *Liometopum* (Lm) by body part, without endosymbionts. Diamonds represent the centroid for each sample type, and line segments connect the centroids to the individual data points.

488 By both Jaccard distance and Bray-Curtis dissimilarity, *Sceptobius* displayed the  
 489 smallest median dissimilarity to *Liometopum*, followed in increasing order by *Myrmecophilus* and  
 490 *Platyusa* (**Fig. 3A**, **Fig. S3**); for this analysis, all sample types except wash samples were  
 491 considered together for each species (for example, *Liometopum* samples included whole body,

492 dissected body, and gut samples). Thus, *Sceptobius* tended to possess the most similar non-  
493 endosymbiotic microbiota to that of its host ant, and *Platyusa* the least similar, regardless of  
494 whether bacterial relative abundances were taken into account. Notably, the same pattern was  
495 also observed for the body wash samples of surface microbiota: following removal of all  
496 ‘background’ environmental ASVs that were present in the nest material samples, we uncovered  
497 the greatest similarity in the surface microbiotas of *Sceptobius* and *Liometopum* (**Fig. 3B**). This  
498 is consistent with direct sharing of stably-associated external microbial symbionts between ants  
499 and socially integrated myrmecophiles—in this case we think driven by ant grooming, and  
500 phoretic attachment of the beetles to workers. The less pronounced but still physically close  
501 interactions between *Myrmecophilus* crickets and *Liometopum* workers also appear to provide  
502 routes for some amount of microbial transfer. Given that host ants outnumber myrmecophiles  
503 by two to three orders of magnitude per nest, it is unlikely that the specific worker ants we  
504 randomly sampled from colonies had recently—if ever—interacted with *Sceptobius* or  
505 *Myrmecophilus*. In contrast, every *Sceptobius* or *Myrmecophilus* individual within a nest is  
506 engaged in constant social interactions with ants. Hence, we propose that the shared microbes  
507 in the ant and myrmecophile samples derive from the ant, rather than the other way around.

508 To gain further resolution into this putative ant-myrmecophile pan-microbiome, we  
509 identified specific ASVs that were shared between specific sets of insect species. Kruskal-Wallis  
510 tests with discrete false discovery rate control (DS-FDR) (Jiang et al., 2017) revealed that 37  
511 ASVs were differentially abundant across *Liometopum*, *Sceptobius*, *Myrmecophilus*, and  
512 *Platyusa* samples (**Table S3**). Among these 37 ASVs, 24 were shared by *Liometopum* and  
513 *Sceptobius*, while 21 were shared by *Liometopum* and *Myrmecophilus*. In contrast, only 10 ASVs  
514 were shared by *Liometopum* and *Platyusa* (**Fig. 3C**). For most of the ASVs shared between  
515 *Liometopum* and either *Sceptobius* or *Myrmecophilus*, the ASVs were more prevalent among the  
516 *Liometopum* samples, implying again that the directionality of microbial sharing tends to be from  
517 ant to myrmecophile rather than vice versa.

518 The results obtained for specific ASVs provide further evidence for microbial sharing  
519 between host ants and myrmecophiles that is correlated with the degree of social interaction  
520 between the insects. We subsequently determined how patterns of microbial sharing between  
521 *Liometopum* and the staphylinids differed by body part, by exploiting *Sceptobius* and *Platyusa*—  
522 the two species that respectively represent the most tightly and weakly integrated  
523 myrmecophiles in this study. Because *Sceptobius* physically interacts with ants using its  
524 mouthparts and legs (Danoff-Burg, 1996), engages in trophallaxis, and because staphylinids in

525 general are capable of pre-oral digestion (Thayer, 2005), we hypothesized that the microbiota of  
526 *Sceptrobius* heads and bodies may exhibit the greatest similarity to the microbiota of the ant.  
527 Consistent with this idea, pairwise Jaccard distances revealed that the microbiota of *Sceptrobius*  
528 heads was indeed the closest among the myrmecophile body parts to ant bodies, followed in  
529 increasing order by *Sceptrobius* bodies and guts (**Fig. 3D**). In contrast, *Platyusa* bodies, guts, and  
530 heads were all significantly less similar to the ant body microbiota than was any single body  
531 region of *Sceptrobius* (**Fig. 3D**). These trends were also recovered in the Jaccard-distance-based  
532 NMDS ordination of ant, *Sceptrobius*, and *Platyusa* samples marked by body part (**Fig. 3E**), and  
533 evident once more via Bray-Curtis dissimilarity (**Fig. S4A**). *Sceptrobius* body parts were also  
534 significantly more similar than *Platyusa* body parts to ant gut samples (**Fig. S4B, C**).

535 That the microbiotas of *Platyusa* and *Liometopum* are more clearly distinct implies that  
536 their transient interactions, via chemical appeasement and predation, do not usually result in  
537 extensive microbial sharing. Interestingly however, using Bray-Curtis dissimilarity, *Platyusa* guts  
538 had a long tail of samples with relatively low dissimilarity to ant bodies and ant wash samples  
539 (**Fig. S4A, D**). This could possibly reflect consumption of host ant workers, but if so, we speculate  
540 that this similarity may reflect transient residents of the *Platyusa* gut rather than true symbionts.  
541 *Sceptrobius* heads and bodies also displayed a tail of relatively low Bray-Curtis dissimilarities to  
542 ant wash samples (**Fig. S4D**). This observation is consistent with microbial sharing between  
543 *Liometopum* and *Sceptrobius* driven at least in part by *Sceptrobius* performing strigilation or  
544 latching onto the ant with its mouthparts, as well as by phoresy.

545 In addition to examining sharing of specific microbial ASVs, we employed weighted  
546 UniFrac to account for phylogenetic relationships between microbial strains present in the  
547 different insect species. Strikingly, weighted UniFrac distances suggested that *Sceptrobius* body  
548 parts were even more similar to ant bodies and guts than was evident from Jaccard distances  
549 or Bray-Curtis dissimilarity. Indeed, by this metric, *Sceptrobius* body parts were roughly as similar  
550 to ant bodies and ant guts as ant bodies and guts were to each other, whereas *Platyusa* body  
551 parts were still significantly more dissimilar to both ant bodies and guts (**Fig. S4E, F**). Given that  
552 UniFrac distances—unlike Jaccard distances or Bray-Curtis dissimilarity—incorporate  
553 phylogenetic information, this finding could potentially suggest an element of convergent  
554 evolution between the microbiotas of *Sceptrobius* and *Liometopum*, on top of direct exchange of  
555 specific microbial species.

## 556 **Myrmecophile microbiota composition is not contingent on deeper evolutionary history**

557 The independent evolution of myrmecophily in the three aleocharine rove beetles enabled us to  
558 ask how these species' microbiotas were contingent on their evolutionary histories as opposed  
559 to their ecologies. The three beetles are inferred to have shared a ~110 million year (MY)-old  
560 free-living common ancestor (Maruyama & Parker, 2017). Subsequently, *Sceptrobius* likely  
561 diverged from its free-living sister, *Lissagria*, ~50 MY ago, but the timing of its ensuing transition  
562 to life in *Liometopum* colonies is uncertain. For *Liometoxenus*, crown-group members of its tribe,  
563 Oxypodini, are inferred to have arisen in the Middle Eocene, implying that *Liometoxenus* is  
564 younger still and that its transition to myrmecophily probably occurred within the past 40 MY  
565 (Maruyama & Parker, 2017). Finally, the three lomechusines, *Drusilla*, *Pella*, and *Platyusa*, share  
566 a common ancestor ~65 MY (Maruyama & Parker, 2017), implying a younger timeframe for  
567 *Platyusa's* association with *Liometopum*. For this analysis, we initially included only the ASVs  
568 classified as putative intracellular endosymbionts, since these are primarily vertically transmitted  
569 (Bright & Bulgheresi, 2010; McCutcheon & Moran, 2012). Furthermore, sequences from such  
570 bacterial symbionts constituted the majority of reads for many of the beetle samples (**Fig. 2A,**  
571 **D**). If evolutionary relationships among the beetles were the main driving factor, due to ancient  
572 acquisition and vertical transmission of endosymbionts, then the myrmecophiles' microbiotas  
573 may be more similar to closely related non-myrmecophilous sister groups than to each other.  
574 Conversely, if a myrmecophilous association with the same *Liometopum* host were a driving  
575 factor, then the myrmecophiles' microbiotas may be more similar to each other.

576 To assess microbiota similarity across the different beetle species, we employed  
577 weighted UniFrac distances (Lozupone, Hamady, Kelley, & Knight, 2007), because we were  
578 interested in the phylogenetic relationships among the endosymbionts. We found that the two  
579 species with the most similar microbiotas by this measure were the *Liometopum* myrmecophiles  
580 *Sceptrobius* and *Platyusa* (**Fig. 4A**). These species showed greater similarity to each other than  
581 to their outgroups, *Lissagria* and *Pella+Drusilla* respectively. However, beyond this relationship,  
582 an obvious pattern was not apparent: for example, the second closest pairing was composed of  
583 *Lissagria* and *Pella*, two phylogenetically distant outgroups, the former a free-living species and  
584 the latter a myrmecophile of *Lasius* ants (**Fig. 4A**). Furthermore, the microbiota of *Liometoxenus*  
585 (tribe Oxypodini) was closest to *Lissagria* (tribe Falagriini) rather than to either *Sceptrobius* or  
586 *Platyusa* with which it coexists in the same host colony (**Fig. 4A**). Examination of the microbiotas  
587 of each staphylinid suggested that these patterns were largely driven by the small numbers of

588 putative endosymbionts associated with each species (**Fig. 4B, C**). For example, both  
589 *Sceptobius* and *Platyusa* possessed only *Rickettsia*, while *Pella* and *Lissagria* possessed  
590 endosymbiont8 and members of the *Rickettsiaceae* family (*Rickettsia* in *Pella* and *Wolbachia* in  
591 *Lissagria*). *Liometoxenus* possessed only endosymbiont8, placing it closer to *Pella* and *Lissagria*  
592 than to *Sceptobius* or *Platyusa*. Finally, *Drusilla* only possessed *Rickettsiella* (a member of the  
593 Gammaproteobacteria and hence more closely related to endosymbiont8 than to *Rickettsia* or  
594 *Wolbachia*).

595 Evidently, the endosymbiotic microbial communities of the three aleocharine members  
596 of the core myrmecophile community cannot be explained by the evolutionary histories of these  
597 beetle species. This qualitative lack of phylosymbiosis—co-cladogenesis between microbial  
598 communities and host organisms—suggests that these putative intracellular endosymbionts  
599 were either acquired after the branching of the different myrmecophiles from outgroups and from  
600 each other, and/or were lost over time in particular lineages. There was likewise no clear effect  
601 of lifestyle on the propensity to possess particular endosymbiont taxa. For example, while  
602 *Sceptobius* and *Platyusa* shared relatively closely related endosymbionts (different *Rickettsia*  
603 ASVs), *Liometoxenus*, which lives with the same host ant species, possessed a very different set  
604 of species. And while *Pella* and *Lissagria* possessed phylogenetically similar endosymbionts, one  
605 is a myrmecophile while the other is free-living. Thus, although our data do not rule out the  
606 possibility that some of the detected putative endosymbionts are a consequence of (or are  
607 adaptive for) a myrmecophilous lifestyle, the acquisition and/or loss of particular clades of  
608 endosymbionts in these staphylinid species may primarily represent chance evolutionary events  
609 within each separate beetle lineage.

610 Finally, we assessed whether there was any evidence for a primary role of ecology versus  
611 evolutionary history among the insects with regard to shaping the composition of their non-  
612 endosymbiont microbiotas. For this analysis, after removing putative intracellular endosymbiont  
613 sequences from the data, we focused on six of the insect species: *Liometopum*, *Sceptobius*,  
614 *Lissagria*, *Platyusa*, *Pella*, and *Lasius*. We hypothesized that if ecology were the primary driver of  
615 the non-endosymbiont microbiotas, the microbiotas of *Platyusa* and *Pella* would be more similar  
616 to that of their ant hosts (*Liometopum* and *Lasius*, respectively) than to that of each other.  
617 Likewise, the microbiota of *Sceptobius* may be more similar to that of *Liometopum* than to that  
618 of its free-living relative, *Lissagria*. Conversely, if the impact of evolutionary history were the  
619 primary driver, *Pella* and *Platyusa* would be more similar to each other than to their ant hosts,  
620 and *Sceptobius* might be more similar to *Lissagria* than to *Liometopum*. Intriguingly, weighted

621 UniFrac distances revealed a trend that was a hybrid of these two scenarios (**Fig. S5**). *Pella* and  
 622 *Platyusa* were indeed more similar to each other than either were to their respective ant hosts,  
 623 and *Lissagria* and *Sceptobius* were also more similar to each other than *Lissagria* was to  
 624 *Liometopum* (which is found in the same region and environments as *Lissagria*, even though the  
 625 two are not behaviorally associated), albeit these trends were not statistically significant. These  
 626 observations suggest a possible influence of shared evolutionary history on the non-  
 627 endosymbiont microbiota of these beetles. Nevertheless, the closest of all the pairings was  
 628 *Sceptobius* and *Liometopum*, suggesting that strong ecological and behavioral ties between  
 629 highly divergent insect species can override this potential phylogenetic effect.

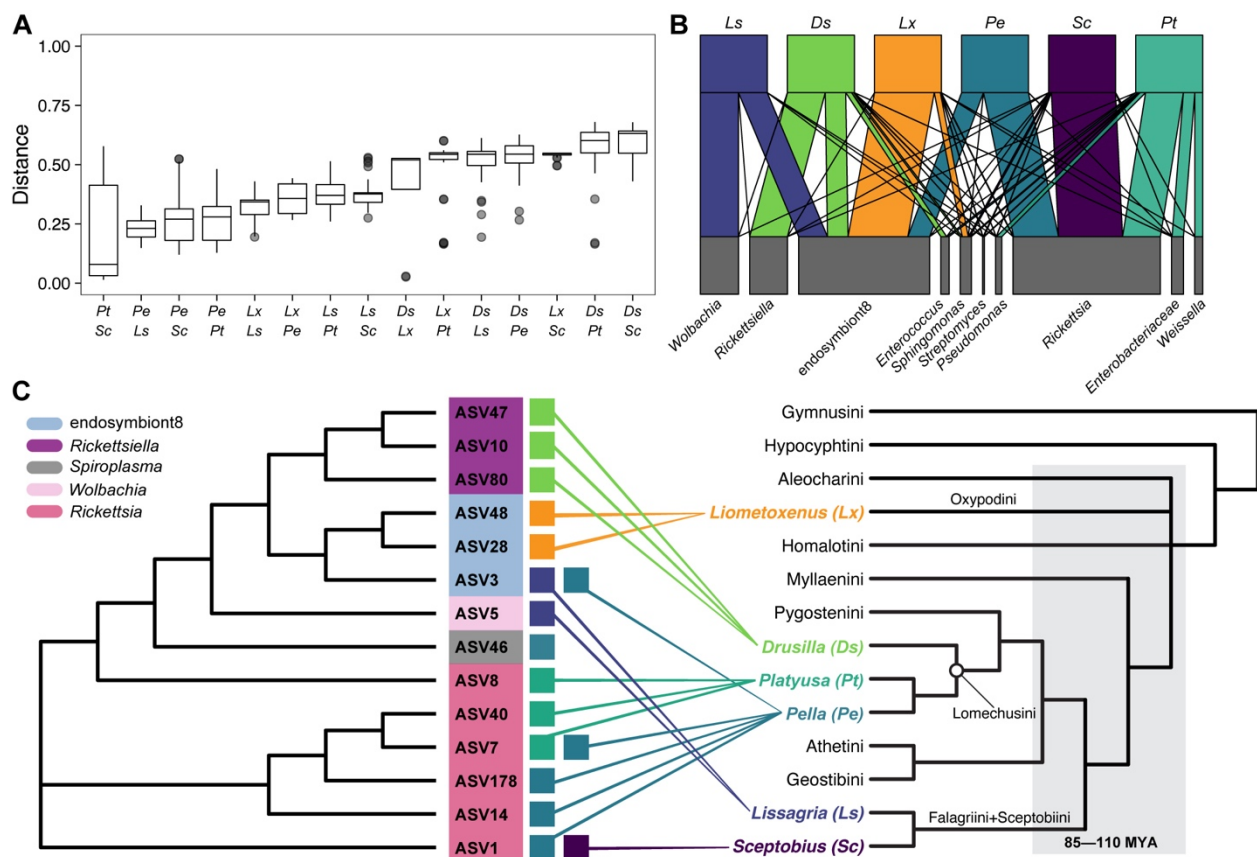


**Figure 4. Relationship between myrmecophile phylogeny and microbiota composition.** **A:** Distributions of weighted UniFrac distances between individuals of different species pairings within the staphylinid beetles in this study. All sample types were included except for wash samples. **B:** Bipartite network plot showing taxonomic overlap of the microbiotas belonging to the different staphylinid beetles. Only the top ten taxa by abundance across these samples are shown. Samples derived from the same species were pooled additively and the taxon abundances were normalized by the number of total reads for each beetle species. **C:** Comparison of the cladogram of the putative endosymbionts associated with the staphylinid beetles and the cladogram of the beetles used in this study together with other major tribes of Aleocharinae, showing a lack of codiversification of the putative endosymbionts with their beetle hosts. The period of extensive tribal-level cladogenesis, 85–110 MY ago, is shaded grey (tree based on Maruyama & Parker, 2017; Orlov, Newton, & Solodovnikov, 2021).

### 630 **Genomic insights into the *Sceptobius* intracellular endosymbiont**

631 Adaptive functions of intracellular endosymbionts are well known in many insect species with  
632 specialized ecologies (Douglas, 1998; McCutcheon, 2021; Zientz et al., 2004). Whether such  
633 endosymbionts might play comparable roles in enabling obligate socially parasitic lifestyles, in  
634 which the insect has sacrificed any capacity for a free-living existence, is, however, unknown.  
635 Such lifestyles commonly involve extreme specialization for life inside host colonies, manifesting  
636 in multiple dimensions of the phenotype including behavior, chemical communication,  
637 reproductive physiology, diet and feeding strategy, as well as morphology. *Sceptobius*  
638 represents a virtuoso example of this type of organism, providing an opportunity to explore  
639 potential microbial involvement in its obligate dependence on *Liometopum* ants. We were struck  
640 by the high abundance of a single *Rickettsia* ASV in all *Sceptobius* samples, at frequencies of up  
641 to 95% of 16S reads per beetle. This bacterium occurred in all beetles of both sexes (importantly,  
642 *Sceptobius* shows no noticeable sex ratio distortion in the populations sampled for this study).  
643 The extreme dominance of this *Rickettsia* species was paired with an absence of other possible  
644 contenders for primary endosymbionts.

645 To shed light on this bacterium—herein named "RiSlat" for "*Rickettsia* endosymbiont of  
646 *Sceptobius lativentris*"—we assembled its genome using Illumina short reads obtained from  
647 genomic DNA extracted from a single male *Sceptobius* body, combined with Oxford Nanopore  
648 long reads from pooled beetles (see Materials and Methods). The final genome assembly  
649 consisted of two contigs with a total size of 1,597,619 bp, and with an average GC content of  
650 32%, typical of Rickettsial genomes (**Table S4**). The completion score was over 99% (**Fig. 5B**)  
651 suggesting that our assembly is a near complete genome. Genomic annotation identified 1825  
652 protein coding sequences with an average size of 741 bp accounting for coding density of circa  
653 85%. Out of the 1825 predicted protein-coding genes, 510 (~30%) were annotated as  
654 hypothetical without known functional domains, while 294 genes (~16%) were predicted to code  
655 for transposases (**Table S4**).

656 The phylogenetic position of the RiSlat in relation to known *Rickettsia* groups was  
657 established based on a concatenated set of 267 single core proteins shared between 86 publicly  
658 available *Rickettsia* genomes. Maximum likelihood analysis placed RiSlat within the "transitional  
659 group" of *Rickettsia*, most closely associated to *Ca. Rickettsia asemboensis* (**Fig. 5A**). The  
660 transitional group is known to host both pathogenic strains, such as *Rickettsia felis*, the causative  
661 agent of a typhus-like flea-borne rickettsiosis (Azad, Radulovic, Higgins, Noden, & Troyer, 1997),  
662 as well as obligate mutualistic endosymbionts including the *Rickettsia* symbiont of the

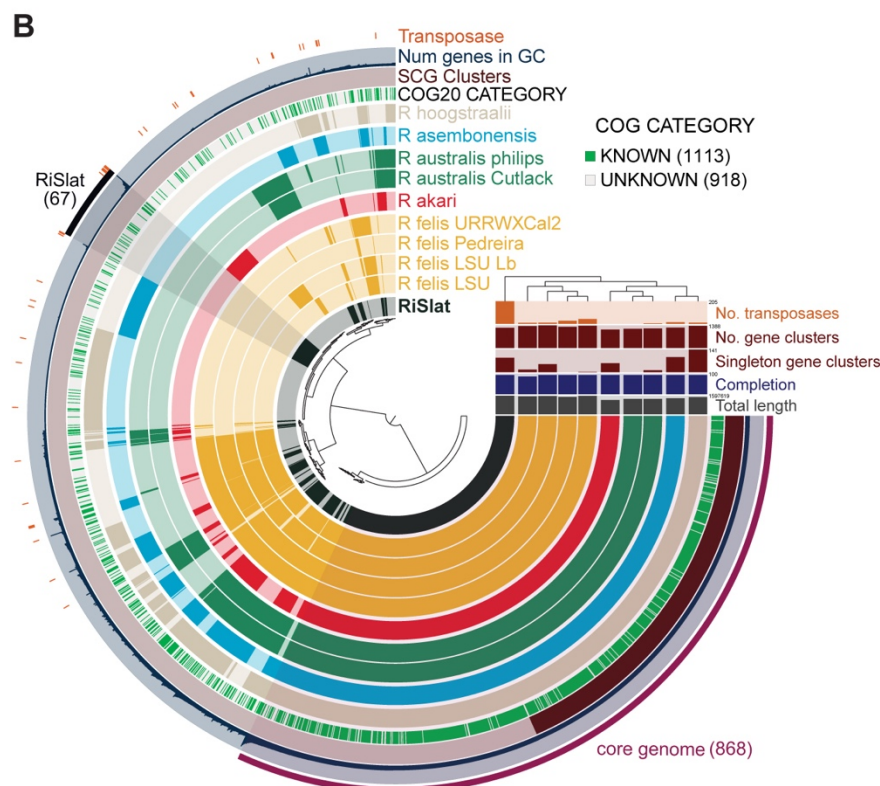
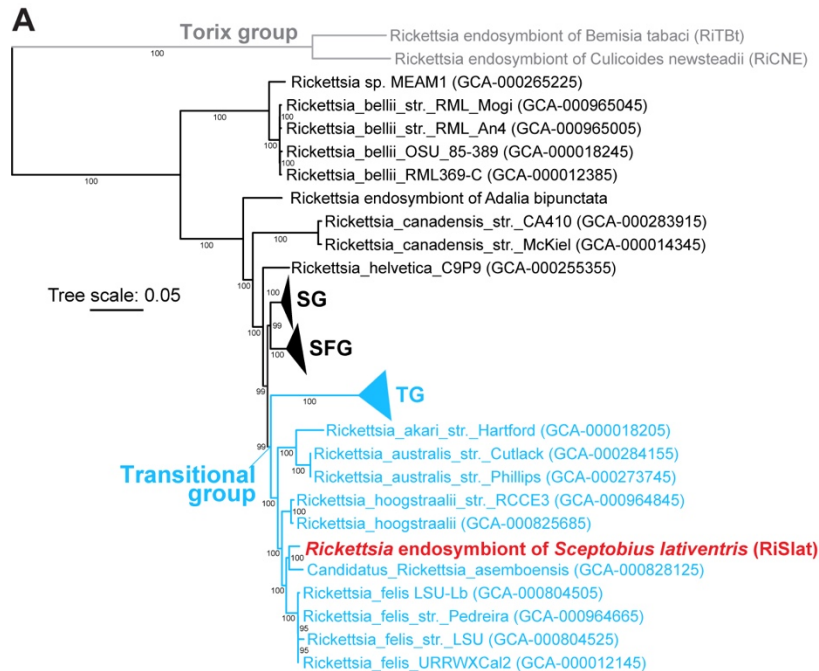


663 parthenogenetic booklouse, *Liposcelis bostrychophila* (Hagimori, Abe, Date, & Miura, 2006;  
664 Perotti, Clarke, Turner, & Braig, 2006; Yusuf & Turner, 2004). We performed a comparative  
665 genomic analysis across members of the transitional group to identify shared and unique  
666 features potentially associated with host specialization and biological function. A total of 2410  
667 gene clusters were identified among the ten available genomes belonging to the transitional  
668 group. 868 of the gene clusters were shared between all genomes, representing the core genome  
669 of the transitional group. Overall, the RiSlat genome shared many of the typical features  
670 associated with the *Rickettsia* genus including a type-IV secretion system, 11 genes coding for  
671 putative surface antigens, and several genes coding for components of toxin-antitoxin systems  
672 (14 toxins and 17 antitoxins). We identified 67 gene clusters comprising a total of 476 genes  
673 specifically associated with the RiSlat genome (**Fig. 5B**). 166 of these genes had at least one  
674 homolog in another *Rickettsia* genome outside of the transitional group, while 310 genes appear  
675 to be uniquely associated with RiSlat (**Table S4**).

676 (Minh et al., 2020)(Eren et al., 2015) Among the RiSlat-specific loci were 113 (~36%) genes with  
677 no assigned function, a toxin-antitoxin pair, and loci encoding a leucine-rich repeat-containing  
678 protein and a D-Ala-D-Ala carboxypeptidase. Most notably, however, 193 genes (~62%) were  
679 annotated as putative transposases belonging to the IS1380 family with a putative gamma-  
680 proteobacterial origin. This large expansion of transposable elements is markedly higher than in  
681 other members of the transitional group (**Fig. 5B**). The majority of these transposases share more  
682 than 95% similarity, suggesting a relatively recent or even an ongoing expansion. Despite their  
683 high number and similarity, we did not detect significant synteny breaks between RiSlat and  
684 other genomes from the transitional group as a result of homologous recombination (**Fig. S6A-**  
685 **D**). Furthermore, the fraction of interrupted genes in RiSlat was estimated to be only ~13.7%  
686 (128 genes with length <80% of their top hit in Swiss-Prot database), which is lower than that of  
687 other members of the transitional group (**Fig. S6E**). This suggests non-significant  
688 pseudogenization despite extensive proliferation of transposable elements.

689 Distant homologs of loci associated with cytoplasmic incompatibility in *Wolbachia* have  
690 been reported in some *Rickettsia* (including the transitional group (Gillespie et al., 2018), but we  
691 find that these are not present in the RiSlat genome. Finally, we assessed the metabolic potential  
692 of the RiSlat genome and compared it to other members of the transitional group by estimating  
693 the completeness of metabolic pathways including carbohydrate and energy metabolism, lipid  
694 and glycan metabolism, amino acid metabolism, and metabolism of cofactors and vitamins (**Fig.**  
695 **S7**). The metabolic potential of RiSlat resembles that of other members of the transitional group.

696 Both cofactors and B vitamin biosynthesis are limited, while most of the amino acid biosynthesis  
 697 pathways are absent or incomplete. These results tentatively argue against a role for RiSlat as a  
 698 nutritional symbiont, and instead indicate that this bacterium may play an alternative role in the  
 699 biology of its host beetle.



700

**Figure 5. Comparative genomics of the *Rickettsia* endosymbiont of *Sceptobius lativentris*.** **A:** Phylogenomic position of *Rickettsia* endosymbiont of *Sceptobius lativentris* (RiSlat) based on concatenated analysis of 267 single copy core proteins. Relationships were inferred using the maximum likelihood criterion as implemented in IQ-TREE 2.0.3 (Minh et al., 2020) under the JTT+F+R5 model. Numbers on branches represent support values based on 1000 ultrafast bootstrap replicates. Some of the *Rickettsia* groups have been collapsed for visualization purposes. SG: Scapularis group; SFG: Spotted fever group; TG: Typhus group. **B:** Comparative genomic analysis across members of the Transitional group of *Rickettsia* using anvi'o package (Eren et al., 2015). Each of the ten inner layers represent the gene clusters (GC) identified in the ten *Rickettsia* genomes and ordered based on their distribution across the ten genomes. *Rickettsia* genomes were clustered and color coded based on gene cluster presence absence (dark color and light color represent presence and absence of a gene cluster). The core genome, the single core genome (SCG) and the gene clusters present only in the *Rickettsia* endosymbiont of *Sceptobius lativentris* (RiSlat) are indicated. Number in the parenthesis correspond to number of gene clusters.

701 **Discussion**

702 We have characterized microbiotas associated with a host ant species and its community of  
703 symbiotic, socially integrated myrmecophiles. Our results shed light on how obligate behavioral  
704 relationships between different animal species can affect their associated microbial communities.  
705 We found that the microbiotas of the host ant and its four core myrmecophiles each display  
706 unique, species-specific characteristics, ranging from the level of taxonomic diversity to the  
707 presence of putative intracellular endosymbionts. Nevertheless, the similarity of the microbiotas  
708 of the different myrmecophiles to that of their common host ant was qualitatively correlated with  
709 each species' level of social interaction with the latter. Moreover, we detected multiple specific  
710 bacterial species that were shared between highly interacting species (e.g. *Liometopum* and  
711 *Sceptobius*) but not between more weakly interacting species (e.g. *Liometopum* and *Platyusa*).  
712 We further identified body part-specific patterns of microbial sharing that match known aspects  
713 of the behavioral interactions between these myrmecophiles species and their host ant. The  
714 patterns of sharing we have uncovered provide evidence for a cross-species pan-microbiome  
715 emerging from close physical relationships between these insect species. Such behaviors  
716 include phoretic attachment to workers, grooming, trophallaxis, and strigilation. Analogues of  
717 these behaviors have evolved convergently in many other ant-myrmecophile relationships, some  
718 of which rank among the most intimate and specialized forms of animal-animal symbiosis  
719 (Hölldobler & Wilson, 1990; Kistner, 1979, 1982; Maruyama et al., 2009; Parker, 2016). We predict  
720 that analogous pan-microbiotas may emerge generally in these contexts of exceptionally close  
721 physical associations between socially integrated myrmecophiles and their hosts.

722 Our findings add to a growing body of evidence that microbial exchange is a pervasive  
723 feature of socially complex metazoan interspecies interactions (Pringle & Moreau, 2017; Song et  
724 al., 2013). To our knowledge, our study is the first to reveal a correlation between the strength of  
725 the social interaction with a given partner (in this case, *Liometopum*), and the degree of microbial  
726 sharing. Whether microbial sharing serves an adaptive function in the context of myrmecophily  
727 is presently unclear. Previous studies have shown how experimentally altering the surface  
728 microbiome of red harvester ants (*Pogonomyrmex barbatus*) leads to increased aggression from  
729 nestmates (Dosmann, Bahet, & Gordon, 2016), implying that ants can either detect differences  
730 in microbial communities, or that microbes modulate the pheromonal chemistry of workers,  
731 perhaps by altering their CHC profiles. Microbial exchange may thus be critical for  
732 myrmecophiles such as *Sceptobius*, which rely on chemical resemblance for social integration,

733 with grooming and close physical contact enabling horizontal acquisition of both CHCs and  
734 surface microbes. The presence of host ant-derived bacteria in the head of *Sceptrobius* may aid  
735 in pre-oral digestion (Thayer, 2005), or be a consequence of strigilation over the ant body surface.  
736 Alternatively, it may arise from the beetle grasping the ant via its mandibles—a stereotyped  
737 behavior that appears to anchor *Sceptrobius* to the worker, freeing up its legs for grooming (**Video**  
738 **S1**).

739 Our findings contrast with a recent survey of microbial diversity in beetles associated with  
740 the red wood ant, *Formica polyctena*, in Europe (Kaczmarczyk-Ziemba, Zagaja, Wagner,  
741 Pietrykowska-Tudruj, & Staniec, 2020). Here, no evidence of microbial sharing was found, but all  
742 the beetle species examined in the study are unspecialized, non-socially integrated taxa that  
743 exhibit no physical interactions with their host ant, perhaps further emphasizing the importance  
744 of behavioral intimacy in establishing a cross-species microbiota. As in our study, Kaczmarczyk-  
745 Ziemba et al (2020) found a high prevalence of putative intracellular endosymbionts among the  
746 staphylinid species. By incorporating multiple rove beetle species that span a range of  
747 phylogenetic relationships and interactions with ants, including outgroup species, we were able  
748 to investigate whether either lifestyle or phylogeny exert a strong influence on these intracellular  
749 bacteria. We conclude that there is little phylogenetic signal in this component of the staphylinid  
750 microbiotas, with little evidence for phylosymbiosis. Although two closely related species,  
751 *Platyusa* and *Pella*, shared the same *Rickettsia* variant (ASV7), other instances of shared  
752 endosymbiont ASVs were between much more distantly related species, such as *Pella* and  
753 *Sceptrobius* (ASV1), or *Pella* and *Lissagria* (ASV3). We also found no clear correlation between  
754 overall intracellular microbiota composition and degree of myrmecophily or the identity of the  
755 host ant species. Together, these results suggest that intracellular endosymbionts, which appear  
756 to dominant the rove beetle microbiota, may have largely been acquired through chance events  
757 in their evolutionary history, rather than reflecting clade-specific physiological factors or selective  
758 pressures imposed by myrmecophily. The lack of conserved taxonomic characteristics among  
759 the different myrmecophile microbiotas does not, however, preclude functional convergence. In  
760 the future, shotgun metagenomic sequencing might reveal whether the latter is indeed the case  
761 among myrmecophiles.

762 Insect endosymbionts are often vertically transmitted, but the lack of a strong  
763 phylogenetic signal in the microbiotas of these staphylinids is perhaps not surprising given that  
764 members of *Rickettsia* and *Wolbachia* (and presumably also *Rickettsiella* and the  
765 “endosymbiont8” clade) are typically facultative endosymbionts. Such bacterial taxa are often

766 not required for the survival of their hosts, and are consequently prone to multiple interspecies  
767 horizontal transfers and losses over evolutionary time (Moran et al., 2008; Perlman, Hunter, &  
768 Zchori-Fein, 2006). The apparent lack of long-term microbial associations in rove beetle  
769 contrasts with other insects where endosymbionts perform vital metabolic functions for their  
770 host insects, the two organisms consequently engaging in pronounced phylosymbiosis (Ivens,  
771 Gadau, Kiers, & Kronauer, 2018). Despite the comparative recency of their associations with rove  
772 beetles, the high within-species prevalence of the most abundant intracellular bacterial species  
773 in our study suggests that some have likely become established as stable, vertically transmitted  
774 endosymbionts. The exact anatomical locations of these bacterial species remain to be  
775 determined, but their broad distributions can be inferred from high abundances across different  
776 dissected beetle body parts. Possible physiological impacts of these microbes are presently  
777 unknown, but facultative endosymbionts generally fall into two categories: those that directly  
778 manipulate reproductive outcomes for their host (e.g. through male killing or cytoplasmic  
779 incompatibility with uninfected mates), and those that offer a mutualistic benefit to their host and  
780 therefore indirectly increase the host's reproductive output (Moran et al., 2008).

781         The high bacterial load and ubiquity of RiSlat in members of both sexes of the *Sceptrobius*  
782 population hints at a potentially beneficial role in the biology of its myrmecophile host. RiSlat  
783 possesses unique genomic features, in particular a large expansion of IS elements of g-  
784 proteobacterial origin, which are not found in other *Rickettsia*. Metabolically, however, RiSlat  
785 largely resembles other members of the transitional group of *Rickettsia*. Importantly, we find no  
786 evidence of nutritional provisioning to the beetle—a phenomenon that has arisen recurrently  
787 across the Coleoptera, in species that feed on nutrient-poor or recalcitrant diets. Microbial  
788 supplementation of tyrosine, which is necessary for formation of the heavily sclerotized beetle  
789 cuticle (Noh, Muthukrishnan, Kramer, & Arakane, 2016), appears in particular to be a relatively  
790 common service provided by beetle endosymbionts (e.g. Anbutsu et al., 2017; Engl et al., 2018;  
791 Vigneron et al., 2014). Although the diet of *Sceptrobius* is not completely known, it likely includes  
792 trophallaxis with host ants and predation on ant brood (Danoff-Burg, 1996)—both of which  
793 represent protein-rich trophic resources. Hence, despite the highly specialized biology of  
794 *Sceptrobius*, we posit that an obligate metabolic dependency on an endosymbiotic bacterium  
795 may not be of relevance, at least during the adult stage.

796         If RiSlat does benefit host biology, we speculate that an alternative role may be as a  
797 defensive symbiont—a function previously ascribed to some non-pathogenic *Rickettsia*  
798 endosymbionts of other insect hosts (Hendry, Hunter, & Baltrus, 2014; Łukasik, Guo, Asch,

799 Ferrari, & Godfray, 2013). The precedent for endosymbionts playing a role in host defense  
800 strategies is particularly intriguing, given that myrmecophilous beetles coexist with aggressive  
801 and chemically defended ants, colonies of which are themselves targeted by a huge diversity of  
802 pathogens and parasites (Bekker, Will, Das, & Adams, 2018; Kistner, 1982; Wojcik, 1989).  
803 Although we detected no consistent correlation between possessing a particular endosymbiont  
804 and having a myrmecophilous lifestyle, different microbial taxa could potentially fulfill similar  
805 functions in different myrmecophiles. Future experiments, including antibiotic treatments to  
806 reduce or eliminate the endosymbiont load, may reveal how these endosymbionts might  
807 contribute to the beetles' fitness in the context of the ant society.

## 808 **Acknowledgments**

809 We thank Clive Turner (UK) for providing living specimens of *Pella cognata* and *Lasius fuliginosus*,  
810 Tim Struyve (Belgium) for providing *Drusilla canaliculata* and Julian Wagner (Caltech) for *Lissagria*  
811 *laeviuscula*. Preliminary stages of this work were facilitated by a seed grant from Caltech's Center  
812 for Environmental Microbial Interactions, and we greatly appreciate the support and generosity  
813 of Dianne Newman (Caltech) throughout the course of this study. This work was funded by an  
814 Army Research Office MURI award, W911NF1910269, to J. Parker.

## 815 **References**

816

- 817 Akino, T. (2002). Chemical camouflage by myrmecophilous beetles *Zyras comes* (Coleoptera:  
818 Staphylinidae) and *Diartiger fossulatus* (Coleoptera: Pselaphidae) to be integrated into the  
819 nest of *Lasius fuliginosus* (Hymenoptera: Formicidae). *Chemoecology*, *12*(2), 83–89.
- 820 Akre, R. D., & Hill, W. B. (1973). Behavior of *Adranes taylori*, a myrmecophilous beetle associated  
821 with *Lasius sitkaensis* in the Pacific Northwest (Coleoptera: Pselaphidae; Hymenoptera: For-  
822 micidae). *Journal of the Kansas Entomological Society*, *46*, 526–536.
- 823 Anbutsu, H., Moriyama, M., Nikoh, N., Hosokawa, T., Futahashi, R., Tanahashi, M., ... Fukatsu,  
824 T. (2017). Small genome symbiont underlies cuticle hardness in beetles. *Proceedings of the*  
825 *National Academy of Sciences*, *114*(40), E8382–E8391. doi: 10.1073/pnas.1712857114
- 826 Azad, A. F., Radulovic, S., Higgins, J. A., Noden, B. H., & Troyer, J. M. (1997). Flea-borne rick-  
827 ettsioses: ecologic considerations. *Emerging Infectious Diseases*, *3*(3), 319–327. doi:  
828 10.3201/eid0303.970308
- 829 Bagnères, A.-G., Blomquist, G. J., Bagnères, A.-G., & Lorenzi, M. C. (2010). *Chemical decep-*  
830 *tion/mimicry using cuticular hydrocarbons*. In *Cambridge Core* (pp. 282–324). Cambridge:  
831 Cambridge University Press. doi: 10.1017/cbo9780511711909.015

- 832 Beeren, C. von, Blüthgen, N., Hoenle, P. O., Pohl, S., Brückner, A., Tishechkin, A. K., ... Kronauer,  
833 D. J. C. (2021). A remarkable legion of guests: Diversity and host specificity of army ant sym-  
834 bionts. *Molecular Ecology*. doi: 10.1111/mec.16101
- 835 Beeren, C. von, Brueckner, A., Maruyama, M., Burke, G., Wieschollek, J., & Kronauer, D. J. C.  
836 (2018). Chemical and behavioral integration of army ant-associated rove beetles - a compar-  
837 ison between specialists and generalists. *Frontiers in Zoology*, 15(1). doi: 10.1186/s12983-  
838 018-0249-x
- 839 Beeren, C. von, Schulz, S., Hashim, R., & Witte, V. (2011). Acquisition of chemical recognition  
840 cues facilitates integration into ant societies. *BMC Ecology*, 11(30), 1–12. doi: 10.1186/1472-  
841 6785-11-30
- 842 Bekker, C. de, Will, I., Das, B., & Adams, R. M. (2018). The ants (Hymenoptera: Formicidae) and  
843 their parasites: effects of parasitic manipulations and host responses on ant behavioral ecol-  
844 ogy. *Myrmecological News*, 28.
- 845 Birtel, J., Walser, J.-C., Pichon, S., Bürgmann, H., & Matthews, B. (2015). Estimating Bacterial  
846 Diversity for Ecological Studies: Methods, Metrics, and Assumptions. *PLoS ONE*, 10(4),  
847 e0125356. doi: 10.1371/journal.pone.0125356
- 848 Bologna, M. A., & Pinto, J. D. (2001). Phylogenetic studies of Meloidae (Coleoptera), with em-  
849 phasis on the evolution of phoresy. *Systematic Entomology*, 26(1), 33–72. doi:  
850 10.1046/j.1365-3113.2001.00132.x
- 851 Bolyen, E., Rideout, J. R., Dillon, M. R., Bokulich, N. A., Abnet, C. C., Al-Ghalith, G. A., ... Capo-  
852 raso, J. G. (2019). Reproducible, interactive, scalable and extensible microbiome data science  
853 using QIIME 2. *Nature Biotechnology*, 37(8), 852–857. doi: 10.1038/s41587-019-0209-9
- 854 Bright, M., & Bulgheresi, S. (2010). A complex journey: transmission of microbial symbionts. *Nature*  
855 *Reviews Microbiology*, 8(3), 218–230. doi: 10.1038/nrmicro2262
- 856 Brooks, A. W., Kohl, K. D., Brucker, R. M., Opstal, E. J. van, & Bordenstein, S. R. (2016). Phylo-  
857 symbiosis: Relationships and Functional Effects of Microbial Communities across Host Evo-  
858 lutionary History. *PLOS Biology*, 14(11), e2000225. doi: 10.1371/journal.pbio.2000225
- 859 Callahan, B. J., McMurdie, P. J., Rosen, M. J., Han, A. W., Johnson, A. J. A., & Holmes, S. P.  
860 (2016). DADA2: High resolution sample inference from Illumina amplicon data. *Nature Meth-*  
861 *ods*, 13(7), 581–583. doi: 10.1038/nmeth.3869
- 862 Cammaerts, R. (1992). Stimuli inducing the regurgitation of the workers of *Lasius flavus* (Formi-  
863 cidae) upon the myrmecophilous beetle *Claviger testaceus* (Pselaphidae). *Behavioural Pro-*  
864 *cesses*, 28(1–2), 81–96.
- 865 Colman, D. R., Toolson, E. C., & Takacs-Vesbach, C. D. (2012). Do diet and taxonomy influence  
866 insect gut bacterial communities? *Molecular Ecology*, 21(20), 5124–5137. doi:  
867 10.1111/j.1365-294x.2012.05752.x

- 868 Danoff-Burg, J. A. (1994). Evolving under myrmecophily: a cladistic revision of the symphilic  
869 beetle tribe Sceptobiini (Coleoptera: Staphylinidae: Aleocharinae). *Systematic Entomology*,  
870 *19*(1), 25–45. doi: 10.1111/j.1365-3113.1994.tb00577.x
- 871 Danoff-Burg, J. A. (1996). An ethogram of the ant-guest beetle tribe Sceptobiini (Coleoptera:  
872 Staphylinidae; Formicidae). *Sociobiology*, *27*(3), 287–328.
- 873 Danoff-Burg, J. A. (2002). Evolutionary Lability and Phylogenetic Utility of Behavior in a Group of  
874 Ant-Guest Staphylinidae Beetles. *Annals of the Entomological Society of America*, *95*(2), 143–  
875 155. doi: 10.1603/0013-8746(2002)095[0143:elapuo]2.0.co;2
- 876 Davis, N. M., Proctor, D. M., Holmes, S. P., Relman, D. A., & Callahan, B. J. (2018). Simple sta-  
877 tistical identification and removal of contaminant sequences in marker-gene and meta-  
878 genomics data. *Microbiome*, *6*(1), 226. doi: 10.1186/s40168-018-0605-2
- 879 Dill-McFarland, K. A., Tang, Z.-Z., Kemis, J. H., Kerby, R. L., Chen, G., Palloni, A., ... Herd, P.  
880 (2019). Close social relationships correlate with human gut microbiota composition. *Scientific*  
881 *Reports*, *9*(1), 703. doi: 10.1038/s41598-018-37298-9
- 882 Dormann, C. F., Gruber, B., & Fründ, J. (2008). Introducing the bipartite package: analysing eco-  
883 logical networks. *Interaction*, *1*(0.2413793).
- 884 Dosmann, A., Bahet, N., & Gordon, D. M. (2016). Experimental modulation of external microbi-  
885 ome affects nestmate recognition in harvester ants (*Pogonomyrmex barbatus*). *PeerJ*, *4*,  
886 e1566. doi: 10.7717/peerj.1566
- 887 Douglas, A. E. (1998). Nutritional Interactions in Insect-Microbial Symbioses: Aphids and Their  
888 Symbiotic Bacteria Buchnera. *Annual Review of Entomology*, *43*(1), 17–37. doi: 10.1146/an-  
889 nurev.ento.43.1.17
- 890 Elmes, G. W., Barr, B., & Thomas, J. A. (1999). Extreme host specificity by *Microdon mutabilis*  
891 (Diptera: Syrphidae), a social parasite of ants. *Proceedings of the Royal Society B: Biological*  
892 *Sciences*, *266*(1418), 447–453. doi: 10.1098/rspb.1999.0658
- 893 Emms, D. M., & Kelly, S. (2019). OrthoFinder: phylogenetic orthology inference for comparative  
894 genomics. *Genome Biology*, *20*(1), 238. doi: 10.1186/s13059-019-1832-y
- 895 Engel, P., & Moran, N. A. (2013). The gut microbiota of insects – diversity in structure and func-  
896 tion. *FEMS Microbiology Reviews*, *37*(5), 699–735. doi: 10.1111/1574-6976.12025
- 897 Engl, T., Eberl, N., Gorse, C., Krüger, T., Schmidt, T. H. P., Plarre, R., ... Kaltenpoth, M. (2018).  
898 Ancient symbiosis confers desiccation resistance to stored grain pest beetles. *Molecular*  
899 *Ecology*, *27*(8), 2095–2108. doi: 10.1111/mec.14418
- 900 Engl, T., & Kaltenpoth, M. (2018). Influence of microbial symbionts on insect pheromones. *Nat-  
901 ural Product Reports*, *35*(5), 386–397. doi: 10.1039/c7np00068e



- 902 Eren, A. M., Esen, Ö. C., Quince, C., Vineis, J. H., Morrison, H. G., Sogin, M. L., & Delmont, T. O.  
903 (2015). Anvi'o: an advanced analysis and visualization platform for 'omics data. *PeerJ*, 3,  
904 e1319. doi: 10.7717/peerj.1319
- 905 Eren, A. M., Kiefl, E., Shaiber, A., Veseli, I., Miller, S. E., Schechter, M. S., ... Willis, A. D. (2021).  
906 Community-led, integrated, reproducible multi-omics with anvi'o. *Nature Microbiology*, 6(1),  
907 3–6. doi: 10.1038/s41564-020-00834-3
- 908 Feener, D. H., & Brown, B. V. (1997). Diptera as parasitoids. *Annual Review of Entomology*, 42(1),  
909 73–97. doi: 10.1146/annurev.ento.42.1.73
- 910 Feldhaar, H., Straka, J., Krischke, M., Berthold, K., Stoll, S., Mueller, M. J., & Gross, R. (2007).  
911 Nutritional upgrading for omnivorous carpenter ants by the endosymbiont Blochmannia. *BMC*  
912 *Biology*, 5(1), 48. doi: 10.1186/1741-7007-5-48
- 913 Gil, R., Silva, F. J., Zientz, E., Delmotte, F., González-Candelas, F., Latorre, A., ... Moya, A. (2003).  
914 The genome sequence of Blochmannia floridanus: Comparative analysis of reduced ge-  
915 nomes. *Proceedings of the National Academy of Sciences*, 100(16), 9388–9393. doi:  
916 10.1073/pnas.1533499100
- 917 Gillespie, J. J., Driscoll, T. P., Verhoeve, V. I., Rahman, M. S., Macaluso, K. R., & Azad, A. F.  
918 (2018). A tangled web: origins of reproductive parasitism. *Genome Biology and Evolution*,  
919 10(9), evy159. doi: 10.1093/gbe/evy159
- 920 Godfray, H. C. J. (1994). *Parasitoids: behavioral and evolutionary ecology* (Vol. 67). Princeton  
921 University Press.
- 922 Grimaldi, D. A., & Engel, M. S. (2005). *Evolution of the Insects*. Cambridge University Press.
- 923 Hagimori, T., Abe, Y., Date, S., & Miura, K. (2006). The First Finding of a Rickettsia Bacterium  
924 Associated with Parthenogenesis Induction Among Insects. *Current Microbiology*, 52(2), 97–  
925 101. doi: 10.1007/s00284-005-0092-0
- 926 Hawkins, B. A. (1994). *Pattern and Process in Host-Parasitoid Interactions*. Cambridge University  
927 Press. doi: 10.1017/cbo9780511721885
- 928 Hebard, M. (1920). A Revision of the North American Species of the Genus Myrmecophila (Or-  
929 thoptera; Gryllidae; Myrmecophilinae). *Transactions of the American Entomological Society*  
930 (1890-), 46(1), 91–111. Retrieved from <http://www.jstor.org/stable/25077026>
- 931 Henderson, G., & Akre, R. D. (1986). Biology of the Myrmecophilous Cricket, *Myrmecophila*  
932 *manni* (Orthoptera: Gryllidae). *Journal of the Kansas Entomological Society*, 59(3), 454–467.  
933 Retrieved from <http://www.jstor.org/stable/25084806>
- 934 Hendry, T. A., Hunter, M. S., & Baltrus, D. A. (2014). The Facultative Symbiont Rickettsia Protects  
935 an Invasive Whitefly against Entomopathogenic *Pseudomonas syringae* Strains. *Applied and*  
936 *Environmental Microbiology*, 80(23), 7161–7168. doi: 10.1128/aem.02447-14

- 937 Hoang, D. T., Chernomor, O., Haeseler, A. von, Minh, B. Q., & Vinh, L. S. (2017). UFBoot2: Im-  
938 proving the Ultrafast Bootstrap Approximation. *Molecular Biology and Evolution*, 35(2), 518–  
939 522. doi: 10.1093/molbev/msx281
- 940 Hoey-Chamberlain, R., Rust, M. K., & Klotz, J. H. (2013). A Review of the Biology, Ecology and  
941 Behavior of Velvety Tree Ants of North America. *Sociobiology*, 60(1), 1–10. doi:  
942 10.1155/1914/69251
- 943 Hölldobler, B. (1967). Zur Physiologie der Gast-Wirt-Beziehungen (Myrmecophilie) bei Ameisen.  
944 I. Das Gastverhältnis der Atermes- und Lomechusa-Larven (Col. Staphylinidae) zu Formica  
945 (Hym. Formicidae)\*. *Zeitschrift für vergleichende Physiologie*, 56(1), 1–21. doi:  
946 10.1007/bf00333561
- 947 Hölldobler, B. (1970). Zur Physiologie der Gast-Wirt-Beziehungen (Myrmecophilie) bei Ameisen.  
948 II. Das Gastverhältnis des imaginalen Atermes pubicollis Bris. (Col. Staphylinidae) zu Myr-  
949 mica und Formica (Hym. Formicidae). *Zeitschrift für vergleichende Physiologie*, 66(2), 215–  
950 250. doi: 10.1007/bf00297780
- 951 Hölldobler, B. (1971). Communication between Ants and Their Guests. *Scientific American*,  
952 224(3), 86–93. doi: 10.1038/scientificamerican0371-86
- 953 Hölldobler, B., & Kwapich, C. L. (2019). Behavior and exocrine glands in the myrmecophilous  
954 beetle *Dinarda dentata* (Gravenhorst, 1806) (Coleoptera: Staphylinidae: Aleocharinae). *PLOS*  
955 *ONE*, 14(1), e0210524-22. doi: 10.1371/journal.pone.0210524
- 956 Hölldobler, B., & Wilson, E. O. (1990). *The Ants*. Harvard University Press.
- 957 Ivens, A. B. F., Gadau, A., Kiers, E. T., & Kronauer, D. J. C. (2018). Can social partnerships influ-  
958 ence the microbiome? Insights from ant farmers and their trophobiont mutualists. *Molecular*  
959 *Ecology*, 27(8), 1898–1914. doi: 10.1111/mec.14506
- 960 Jennings, E. C., Korthauer, M. W., Hamilton, T. L., & Benoit, J. B. (2019). Matrotrophic viviparity  
961 constrains microbiome acquisition during gestation in a live-bearing cockroach, *Diploptera*  
962 *punctata*. *Ecology and Evolution*, 9(18), 10601–10614. doi: 10.1002/ece3.5580
- 963 Jiang, L., Amir, A., Morton, J. T., Heller, R., Arias-Castro, E., & Knight, R. (2017). Discrete False-  
964 Discovery Rate Improves Identification of Differentially Abundant Microbes. *MSystems*, 2(6),  
965 e00092-17. doi: 10.1128/msystems.00092-17
- 966 Jones, P., Binns, D., Chang, H.-Y., Fraser, M., Li, W., McAnulla, C., ... Hunter, S. (2014). Inter-  
967 ProScan 5: genome-scale protein function classification. *Bioinformatics*, 30(9), 1236–1240.  
968 doi: 10.1093/bioinformatics/btu031
- 969 Jones, R. T., Sanchez, L. G., & Fierer, N. (2013). A Cross-Taxon Analysis of Insect-Associated  
970 Bacterial Diversity. *PLoS ONE*, 8(4), e61218. doi: 10.1371/journal.pone.0061218

- 971 Jordan, K. (1913). Zur Morphologie und Biologie der myrmecophilen Gattungen *Lomechusa* und  
972 *Atemeles* und einiger verwandter Formen. *Zeitschrift Für Wissenschaftliche Zoologie*, 107,  
973 346–386.
- 974 Kaczmarczyk-Ziemia, A., Zagaja, M., Wagner, G. K., Pietrykowska-Tudruj, E., & Staniec, B.  
975 (2020). First Insight into Microbiome Profiles of Myrmecophilous Beetles and Their Host, Red  
976 Wood Ant *Formica polyctena* (Hymenoptera: Formicidae)—A Case Study. *Insects*, 11(2), 134.  
977 doi: 10.3390/insects11020134
- 978 Kaltenpoth, M., & Engl, T. (2014). Defensive microbial symbionts in Hymenoptera. *Functional*  
979 *Ecology*, 28(2), 315–327. doi: 10.1111/1365-2435.12089
- 980 Kalyaanamoorthy, S., Minh, B. Q., Wong, T. K. F., Haeseler, A. von, & Jermini, L. S. (2017). Mod-  
981 elFinder: fast model selection for accurate phylogenetic estimates. *Nature Methods*, 14(6),  
982 587–589. doi: 10.1038/nmeth.4285
- 983 Kang, D. D., Li, F., Kirton, E., Thomas, A., Egan, R., An, H., & Wang, Z. (2019). MetaBAT 2: an  
984 adaptive binning algorithm for robust and efficient genome reconstruction from metagenome  
985 assemblies. *PeerJ*, 7, e7359. doi: 10.7717/peerj.7359
- 986 Kathirithamby, J. (2009). Host-Parasitoid Associations in Strepsiptera. *Annual Review of Ento-*  
987 *mology*, 54(1), 227–249. doi: 10.1146/annurev.ento.54.110807.090525
- 988 Kistner, D. H. (1979). *Social and evolutionary significance of social insect symbionts* (H. R. Her-  
989 mann, Ed.). In *Vol. I* (pp. 339–413).
- 990 Kistner, D. H. (1982). *The Social Insects' Bestiary* (H. R. Hermann, Ed.). In (pp. 1–244).
- 991 Koch, H., & Schmid-Hempel, P. (2011). Socially transmitted gut microbiota protect bumble bees  
992 against an intestinal parasite. *Proceedings of the National Academy of Sciences*, 108(48),  
993 19288–19292. doi: 10.1073/pnas.1110474108
- 994 Kolde, R., & Kolde, M. R. (2015). Package 'pheatmap.' *R Package*, 1(7), 790.
- 995 Komatsu, T., Maruyama, M., & Itino, T. (2009). Behavioral differences between two ant cricket  
996 species in Nansei Islands: host-specialist versus host-generalist. *Insectes Sociaux*, 56(4),  
997 389–396. doi: 10.1007/s00040-009-0036-y
- 998 Kovarik, P. W., & Caterino, M. S. (2005). *Histeridae Gyllenhal, 1808* (R. G. Beutel & R. A. B.  
999 Leschen, Eds.). In (pp. 190–222). Walter de Gruyter.
- 1000 Kurtz, S., Phillippy, A., Delcher, A. L., Smoot, M., Shumway, M., Antonescu, C., & Salzberg, S.  
1001 L. (2004). Versatile and open software for comparing large genomes. *Genome Biology*, 5(2),  
1002 R12. doi: 10.1186/gb-2004-5-2-r12
- 1003 Lenoir, A., Chalon, Q., Carvajal, A., Ruel, C., Barroso, Á., Lackner, T., & Boulay, R. (2012). Chem-  
1004 ical Integration of Myrmecophilous Guests in *Aphaenogaster* Ant Nests. *Psyche: A Journal of*  
1005 *Entomology*, 2012, 1–12. doi: 10.1155/2012/840860

- 1006 Leschen, R. A. B. (1991). Behavioral observations on the myrmecophile *Fustiger knausii* (Coleoptera: Pselaphidae: Clavigerinae) with a discussion of grasping notches in myrmecophiles. *Entomological News*, 102(5), 215–222.
- 1007  
1008
- 1009 Letunic, I., & Bork, P. (2007). Interactive Tree Of Life (iTOL): an online tool for phylogenetic tree display and annotation. *Bioinformatics*, 23(1), 127–128. doi: 10.1093/bioinformatics/btl529
- 1010
- 1011 Li, D., Liu, C.-M., Luo, R., Sadakane, K., & Lam, T.-W. (2015). MEGAHIT: an ultra-fast single-node solution for large and complex metagenomics assembly via succinct de Bruijn graph. *Bioinformatics*, 31(10), 1674–1676. doi: 10.1093/bioinformatics/btv033
- 1012  
1013
- 1014 Li, H. (2018). Minimap2: pairwise alignment for nucleotide sequences. *Bioinformatics*, 34(18), 3094–3100. doi: 10.1093/bioinformatics/bty191
- 1015
- 1016 Li, H., Handsaker, B., Wysoker, A., Fennell, T., Ruan, J., Homer, N., ... Subgroup, 1000 Genome Project Data Processing. (2009). The Sequence Alignment/Map format and SAMtools. *Bioinformatics*, 25(16), 2078–2079. doi: 10.1093/bioinformatics/btp352
- 1017  
1018
- 1019 López-Estrada, E. K., Sanmartín, I., Uribe, J. E., Abalde, S., & García-París, M. (2021). Diversification dynamics of hypermetamorphic blister beetles (Meloidae): Are homoplastic host shifts and phoresy key factors of a rushing forward strategy to escape extinction? *BioRxiv*, 2021.01.04.425192. doi: 10.1101/2021.01.04.425192
- 1020  
1021  
1022
- 1023 Lozupone, C. A., Hamady, M., Kelley, S. T., & Knight, R. (2007). Quantitative and Qualitative  $\beta$  Diversity Measures Lead to Different Insights into Factors That Structure Microbial Communities. *Applied and Environmental Microbiology*, 73(5), 1576–1585. doi: 10.1128/aem.01996-06
- 1024  
1025  
1026
- 1027 Łukasik, P., Guo, H., Asch, M., Ferrari, J., & Godfray, H. C. J. (2013). Protection against a fungal pathogen conferred by the aphid facultative endosymbionts *Rickettsia* and *Spiroplasma* is expressed in multiple host genotypes and species and is not influenced by co-infection with another symbiont. *Journal of Evolutionary Biology*, 26(12), 2654–2661. doi: 10.1111/jeb.12260
- 1028  
1029  
1030
- 1031 Majumder, R., Sutcliffe, B., Adnan, S. M., Mainali, B., Dominiak, B. C., Taylor, P. W., & Chapman, T. A. (2020). Artificial Larval Diet Mediates the Microbiome of Queensland Fruit Fly. *Frontiers in Microbiology*, 11, 576156. doi: 10.3389/fmicb.2020.576156
- 1032  
1033
- 1034 Maruyama, M., Akino, T., Hashim, R., & Komatsu, T. (2009). Behavior and cuticular hydrocarbons of myrmecophilous insects (Coleoptera: Staphylinidae; Diptera: Phoridae; Thysanura) associated with Asian *Aenictus* army ants (Hymenoptera; Formicidae). *Sociobiology*, 54(1), 19–35.
- 1035  
1036
- 1037 Maruyama, M., & Parker, J. (2017). Deep-Time Convergence in Rove Beetle Symbionts of Army Ants. *Current Biology*, 27(6), 920–926. doi: 10.1016/j.cub.2017.02.030
- 1038
- 1039 Mason, C. J., Clair, A. St., Peiffer, M., Gomez, E., Jones, A. G., Felton, G. W., & Hoover, K. (2020). Diet influences proliferation and stability of gut bacterial populations in herbivorous lepidopteran larvae. *PLOS ONE*, 15(3), e0229848. doi: 10.1371/journal.pone.0229848
- 1040  
1041

- 1042 McCutcheon, J. P. (2021). The Genomics and Cell Biology of Host-Beneficial Intracellular Infec-  
1043 tions. *Annual Review of Cell and Developmental Biology*, 37(1), 1–28. doi: 10.1146/annurev-  
1044 cellbio-120219-024122
- 1045 McCutcheon, J. P., & Moran, N. A. (2012). Extreme genome reduction in symbiotic bacteria.  
1046 *Nature Reviews Microbiology*, 10(1), 13–26. doi: 10.1038/nrmicro2670
- 1047 McMurdie, P. J., & Holmes, S. (2013). phyloseq: An R Package for Reproducible Interactive Anal-  
1048 ysis and Graphics of Microbiome Census Data. *PLoS ONE*, 8(4), e61217. doi: 10.1371/jour-  
1049 nal.pone.0061217
- 1050 Meer, R. K. V., & Wojcik, D. P. (1982). Chemical Mimicry in the Myrmecophilous Beetle Myrmec-  
1051 aphodius excavaticollis. *Science*, 218(4574), 806–808. doi: 10.1126/science.218.4574.806
- 1052 Minh, B. Q., Schmidt, H. A., Chernomor, O., Schrempf, D., Woodhams, M. D., Haeseler, A. von,  
1053 & Lanfear, R. (2020). IQ-TREE 2: New models and efficient methods for phylogenetic inference  
1054 in the genomic era. *Molecular Biology and Evolution*, 37(5), 1530–1534. doi: 10.1093/mol-  
1055 bev/msaa015
- 1056 Moeller, A. H., Foerster, S., Wilson, M. L., Pusey, A. E., Hahn, B. H., & Ochman, H. (2016). Social  
1057 behavior shapes the chimpanzee pan-microbiome. *Science Advances*, 2(1), e1500997. doi:  
1058 10.1126/sciadv.1500997
- 1059 Moran, N. A., McCutcheon, J. P., & Nakabachi, A. (2008). Genomics and evolution of heritable  
1060 bacterial symbionts. *Annual Review of Genetics*, 42(1), 165–190. doi: 10.1146/an-  
1061 nurev.genet.41.110306.130119
- 1062 Morton, W., William. (1900). The Habits of Myrmecophila Nebrascensis Bruner. *Psyche: A Jour-  
1063 nal of Entomology*, 9(294), 111–115. doi: 10.1155/1900/75323
- 1064 Noh, M. Y., Muthukrishnan, S., Kramer, K. J., & Arakane, Y. (2016). Cuticle formation and pig-  
1065 mentation in beetles. *Current Opinion in Insect Science*, 17, 1–9. doi:  
1066 10.1016/j.cois.2016.05.004
- 1067 Ogle, D., Wheeler, P., & Dinno, A. (2020). FSA: fisheries stock analysis. R package version 0.8.  
1068 30. Retrived from <https://Github.Com/Droglenc/FSA>.
- 1069 Oksanen, J., Blanchet, F. G., Kindt, R., Legendre, P., Minchin, P., O’Hara, R., ... others. (2015).  
1070 Vegan community ecology package: ordination methods, diversity analysis and other func-  
1071 tions for community and vegetation ecologists. *R Package Ver*, 2–3.
- 1072 Oliver, K. M., Russell, J. A., Moran, N. A., & Hunter, M. S. (2003). Facultative bacterial symbionts  
1073 in aphids confer resistance to parasitic wasps. *Proceedings of the National Academy of Sci-  
1074 ences*, 100(4), 1803–1807. doi: 10.1073/pnas.0335320100
- 1075 Orlov, I., Newton, A. F., & Solodovnikov, A. (2021). Phylogenetic review of the tribal system of  
1076 Aleocharinae, a mega-lineage of terrestrial arthropods in need of reclassification. *Journal of  
1077 Zoological Systematics and Evolutionary Research*. doi: 10.1111/jzs.12524

- 1078 Park, R., Dzialo, M. C., Spaepen, S., Nsabimana, D., Gielens, K., Devriese, H., ... Verstrepen, K.  
1079 J. (2019). Microbial communities of the house fly *Musca domestica* vary with geographical  
1080 location and habitat. *Microbiome*, 7(1), 147. doi: 10.1186/s40168-019-0748-9
- 1081 Parker, J. (2016). Myrmecophily in beetles (Coleoptera): evolutionary patterns and biological  
1082 mechanisms. *Myrmecological News*, 22, 65–108.
- 1083 Parker, J., & Grimaldi, D. A. (2014). Specialized Myrmecophily at the Ecological Dawn of Modern  
1084 Ants. *Current Biology*, 24(20), 2428–2434. doi: 10.1016/j.cub.2014.08.068
- 1085 Parker, J., & Kronauer, D. J. C. (2021). How ants shape biodiversity. *Current Biology*.
- 1086 Parks, D. H., Imelfort, M., Skennerton, C. T., Hugenholtz, P., & Tyson, G. W. (2015). CheckM:  
1087 assessing the quality of microbial genomes recovered from isolates, single cells, and meta-  
1088 genomes. *Genome Research*, 25(7), 1043–1055. doi: 10.1101/gr.186072.114
- 1089 Perlman, S. J., Hunter, M. S., & Zchori-Fein, E. (2006). The emerging diversity of Rickettsia. *Pro-  
1090 ceedings of the Royal Society B: Biological Sciences*, 273(1598), 2097–2106. doi:  
1091 10.1098/rspb.2006.3541
- 1092 Perotti, M. A., Clarke, H. K., Turner, B. D., & Braig, H. R. (2006). Rickettsia as obligate and my-  
1093 cetomic. *The FASEB Journal*, 20(13), 2372–2374. doi: 10.1096/fj.06-5870fje
- 1094 Piel, J. (2002). A polyketide synthase-peptide synthetase gene cluster from an uncultured bac-  
1095 terial symbiont of *Paederus* beetles. *Proceedings of the National Academy of Sciences of the  
1096 United States of America*, 99(22), 14002–14007. doi: 10.1073/pnas.222481399
- 1097 Pierce, N. E., Braby, M. F., Heath, A., Lohman, D. J., Mathew, J., Rand, D. B., & Travassos, M.  
1098 A. (2002). The ecology and evolution of ant association in the Lycaenidae (Lepidoptera). *An-  
1099 nual Review of Entomology*, 47, 733–771. doi: 10.1146/annurev.ento.47.091201.145257
- 1100 Quast, C., Pruesse, E., Yilmaz, P., Gerken, J., Schweer, T., Yarza, P., ... Glöckner, F. O. (2013).  
1101 The SILVA ribosomal RNA gene database project: improved data processing and web-based  
1102 tools. *Nucleic Acids Research*, 41(D1), D590–D596. doi: 10.1093/nar/gks1219
- 1103 Renelies-Hamilton, J., Germer, K., Sillam-Dussès, D., Bodawatta, K. H., & Poulsen, M. (2021).  
1104 Disentangling the Relative Roles of Vertical Transmission, Subsequent Colonizations, and  
1105 Diet on Cockroach Microbiome Assembly. *MSphere*, 6(1). doi: 10.1128/msphere.01023-20
- 1106 Russell, J. A., Moreau, C. S., Goldman-Huertas, B., Fujiwara, M., Lohman, D. J., & Pierce, N. E.  
1107 (2009). Bacterial gut symbionts are tightly linked with the evolution of herbivory in ants. *Pro-  
1108 ceedings of the National Academy of Sciences*, 106(50), 21236–21241. doi:  
1109 10.1073/pnas.0907926106
- 1110 Salem, H., Bauer, E., Kirsch, R., Berasategui, A., Cripps, M., Weiss, B., ... Kaltenpoth, M. (2017).  
1111 Drastic Genome Reduction in an Herbivore's Pectinolytic Symbiont. *Cell*, 1–26. doi:  
1112 10.1016/j.cell.2017.10.029

- 1113 Salter, S. J., Cox, M. J., Turek, E. M., Calus, S. T., Cookson, W. O., Moffatt, M. F., ... Walker, A.  
1114 W. (2014). Reagent and laboratory contamination can critically impact sequence-based mi-  
1115 crobiome analyses. *BMC Biology*, *12*(1), 87. doi: 10.1186/s12915-014-0087-z
- 1116 Scudder, G. G. E. (2017). The Importance of Insects. In R. G. Foottit & P. H. Adler (Eds.), *Insect*  
1117 *Biodiversity: Science and Society* (pp. 9–43). John Wiley & Sons. doi:  
1118 10.1002/9781118945568.ch2
- 1119 Seemann, T. (2014). Prokka: rapid prokaryotic genome annotation. *Bioinformatics*, *30*(14), 2068–  
1120 2069. doi: 10.1093/bioinformatics/btu153
- 1121 Seevers, C. H. (1965). The systematics, evolution and zoogeography of staphylinid beetles as-  
1122 sociated with army ants (Coleoptera, Staphylinidae). *Fieldiana Zoology*, *47*(2), 139–351.
- 1123 Song, S. J., Lauber, C., Costello, E. K., Lozupone, C. A., Humphrey, G., Berg-Lyons, D., ...  
1124 Knight, R. (2013). Cohabiting family members share microbiota with one another and with  
1125 their dogs. *ELife*, *2*, e00458. doi: 10.7554/elife.00458
- 1126 Stadler, B., & Dixon, A. F. G. (2005). Ecology and Evolution of Aphid-Ant Interactions. *Annual*  
1127 *Review of Ecology, Evolution, and Systematics*, *36*, 345–372.
- 1128 Stoeffler, M., Tolasch, T., & Steidle, J. L. M. (2011). Three beetles—three concepts. Different  
1129 defensive strategies of congeneric myrmecophilous beetles. *Behavioral Ecology and Socio-*  
1130 *biology*, *65*(8), 1605–1613. doi: 10.1007/s00265-011-1171-9
- 1131 Strand, M. R., & Obrycki, J. J. (1996). Host Specificity of Insect Parasitoids and Predators Many  
1132 factors influence the host ranges of insect natural enemies. *BioScience*, *46*(6), 422–429. doi:  
1133 10.2307/1312876
- 1134 Thayer, M. K. (2005). *Staphylinidae Latreille, 1802* (R. G. Beutel & R. A. B. Leschen, Eds.). In (pp.  
1135 296–344). Walter de Gruyter.
- 1136 Tung, J., Barreiro, L. B., Burns, M. B., Grenier, J.-C., Lynch, J., Grieneisen, L. E., ... Archie, E. A.  
1137 (2015). Social networks predict gut microbiome composition in wild baboons. *ELife*, *4*,  
1138 e05224. doi: 10.7554/elife.05224
- 1139 Ul-Hasan, S., Bowers, R. M., Figueroa-Montiel, A., Licea-Navarro, A. F., Beman, J. M., Woyke,  
1140 T., & Nobile, C. J. (2019). Community ecology across bacteria, archaea and microbial eukar-  
1141 yotes in the sediment and seawater of coastal Puerto Nuevo, Baja California. *PLOS ONE*,  
1142 *14*(2), e0212355. doi: 10.1371/journal.pone.0212355
- 1143 Vigneron, A., Masson, F., Vallier, A., Balmand, S., Rey, M., Vincent-Monégat, C., ... Heddi, A.  
1144 (2014). Insects Recycle Endosymbionts when the Benefit Is Over. *Current Biology*, *24*(19),  
1145 2267–2273. doi: 10.1016/j.cub.2014.07.065
- 1146 Wada-Katsumata, A., Zurek, L., Nalyanya, G., Roelofs, W. L., Zhang, A., & Schal, C. (2015). Gut  
1147 bacteria mediate aggregation in the German cockroach. *Proceedings of the National Acad-*  
1148 *emy of Sciences*, *112*(51), 15678–15683. doi: 10.1073/pnas.1504031112

- 1149 Wang, T. B., Patel, A., Vu, F., & Nonacs, P. (2010). Natural History Observations on the Velvety  
1150 Tree Ant (*Liometopum occidentale*): Unicoloniality and Mating Flights. *Sociobiology*, 55(3),  
1151 787–794. doi: 10.1111/j.1558-5646.2009.00628.x
- 1152 Wick, R. R., Judd, L. M., Gorrie, C. L., & Holt, K. E. (2017). Unicycler: Resolving bacterial genome  
1153 assemblies from short and long sequencing reads. *PLOS Computational Biology*, 13(6),  
1154 e1005595. doi: 10.1371/journal.pcbi.1005595
- 1155 Wickham, H. (2011). ggplot2. *Wiley Interdisciplinary Reviews: Computational Statistics*, 3(2), 180–  
1156 185.
- 1157 Wojcik, D. P. (1989). Behavioral Interactions between Ants and Their Parasites. *The Florida En-*  
1158 *tomologist*, 72(1), 43–51. doi: 10.2307/3494966?ref=no-x-  
1159 route:2d46a42242f93ba50fee4895d3959302
- 1160 Yamamoto, S., Maruyama, M., & Parker, J. (2016). Evidence for social parasitism of early insect  
1161 societies by Cretaceous rove beetles. *Nature Communications*, 7, 13658. doi:  
1162 10.1038/ncomms13658
- 1163 Yun, J.-H., Roh, S. W., Whon, T. W., Jung, M.-J., Kim, M.-S., Park, D.-S., ... Bae, J.-W. (2014).  
1164 Insect Gut Bacterial Diversity Determined by Environmental Habitat, Diet, Developmental  
1165 Stage, and Phylogeny of Host. *Applied and Environmental Microbiology*, 80(17), 5254–5264.  
1166 doi: 10.1128/aem.01226-14
- 1167 Yusuf, M., & Turner, B. (2004). Characterisation of Wolbachia-like bacteria isolated from the par-  
1168 thenogenetic stored-product pest psocid *Liposcelis bostrychophila* (Badonnel) (Psocoptera).  
1169 *Journal of Stored Products Research*, 40(2), 207–225. doi: 10.1016/s0022-474x(02)00098-x
- 1170 Zientz, E., Dandekar, T., & Gross, R. (2004). Metabolic Interdependence of Obligate Intracellular  
1171 Bacteria and Their Insect Hosts†. *Microbiology and Molecular Biology Reviews*, 68(4), 745–  
1172 770. doi: 10.1128/mnbr.68.4.745-770.2004
- 1173



1174 **Supplemental figure legends**

1175 **Figure S1.** Bar plots showing relative abundance of different bacterial taxa in individual samples  
1176 of the studied species. *Lm* = *Liometopum* (ant), *Mm* = *Myrmecophilus* (cricket), *Sc* = *Sceptobius*  
1177 (beetle), *Lx* = *Liometoxenus* (beetle), *Pt* = *Platyusa* (beetle), *Pe* = *Pella* (beetle), *La* = *Lasius* (ant),  
1178 *Ds* = *Drusilla* (beetle), *Ls* = *Lissagria* (beetle), WB = whole body.

1179 **Figure S2. A:** NMDS ordination of nest and wash samples, based on Jaccard distance or Bray-  
1180 Curtis dissimilarity and colored by nest site. Note that in some cases, individual samples are  
1181 obscured by their proximity to each other or to the group centroid. **B:** Pairwise Jaccard distances  
1182 and Bray-Curtis dissimilarities for wash samples and body part samples versus nest samples.

1183 **Figure S3.** Bray-Curtis pairwise dissimilarities for *Sceptobius* (*Sc*), *Platyusa* (*Pt*), and  
1184 *Myrmecophilus* (*Mm*) versus *Liometopum*, within nest sites, without endosymbionts. All sample  
1185 types except wash samples (i.e. whole body samples in addition to dissected body parts where  
1186 applicable) were included for each species.

1187 **Figure S4.** Pairwise distances or dissimilarities between different myrmecophile body parts and  
1188 ant body parts, without endosymbionts. **A:** Bray-Curtis dissimilarities versus ant bodies. **B:** Bray-  
1189 Curtis dissimilarities versus ant guts. **C:** Jaccard distances versus ant guts. **D:** Bray-Curtis  
1190 dissimilarities versus ant wash samples. **E:** Weighted UniFrac distances versus ant bodies. **F:**  
1191 Weighted UniFrac distances versus ant guts.

1192 **Figure S5.** Pairwise weighted UniFrac distances between different staphylinids and ant species,  
1193 without endosymbionts. All sample types were included except for wash samples.

1194 **Figure S6. A-C:** Syntenic comparison between RiSlat and related and complete genomes from  
1195 the transitional group of *Rickettsia*. **D:** Mummer self-plots representing the repeat density  
1196 ( $\geq 1500$ bp and  $\geq 95\%$  similarity) in the RiSlat genome. Magenta represents forward matches and  
1197 blue represents reverse matches. **E:** Fraction of interrupted genes in RiSlat genome in  
1198 comparison to other genomes from transitional group.

1199  
1200 **Figure S7.** Reconstruction and comparative analysis of the metabolic potential across  
1201 Transitional group *Rickettsia*. Pathway completeness for different KEGG functional categories  
1202 were estimated using the “anvi-estimate-metabolism” program from the anvi'o package.

1203 **Supplemental Videos**

1204 **Video S1.** A *Sceptobius lativentris* beetle mounted on top of a *Liometopum occidentale* worker.  
1205 The beetle grasps the ant's antenna in its mandibles and uses its tarsi to groom the ant's body  
1206 surface before smearing its tarsi over its own body. Grooming behavior transfers cuticular  
1207 hydrocarbon pheromones from the ant onto the beetle. Video shot under infrared illumination at  
1208 90 frames per second.

1209 **Supplemental Tables**

1210 **Table S1.** The frequency of each ASV per sample (normalized to 1000 reads). Mean frequencies  
1211 per sample type, as well as sample metadata, are provided as separate tabs within this table.

1212 **Table S2.** Summary of statistical tests used in this paper.

1213 **Table S3.** Kruskal-Wallis test statistics and raw *p*-values for the 37 ASVs that were identified as  
1214 differentially abundant across *Liometopum*, *Sceptobius*, *Myrmecophilus*, and *Platyusa* after  
1215 using DS-FDR to control the false discovery rate. The order of the rows is the same as for the  
1216 heatmap shown in **Fig. 3C**.

1217 **Table S4.** Genome features of the *Rickettsia* endosymbiont of *Sceptobius lativentris* (RiSlat).

Total size (bp)	1,597,619
Number of contigs	2
Largest contig (bp)	1,551,323
Average coverage per contig	contig_1: 85x, contig_2: 161x
GC contents (%)	32
Number of predicted CDS	1825
Average CDS length (bp)	741
Number of rRNAs	3
Number of tRNAs	34
Plasmids	Contig_2 is a possible low copy plasmid

1218 **Table S5.** Genome annotation file for the *Rickettsia* endosymbiont of *Sceptobius lativentris*  
1219 (RiSlat).

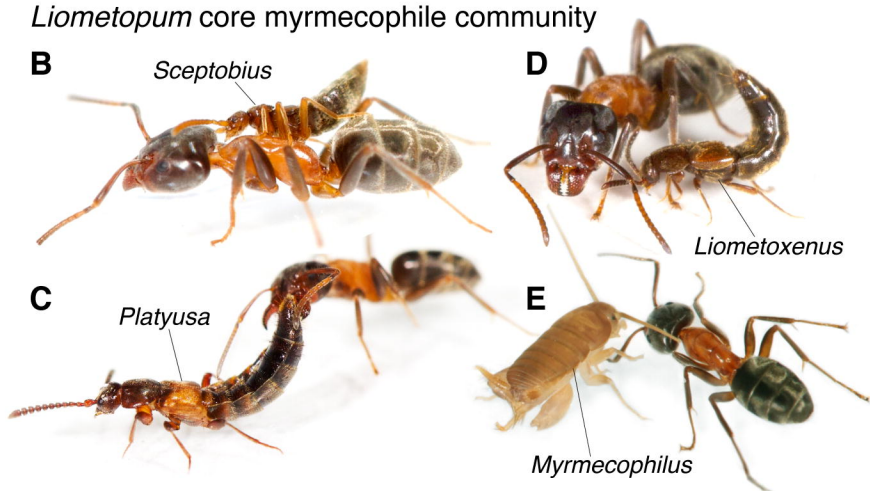
1220 **Supplemental Files**

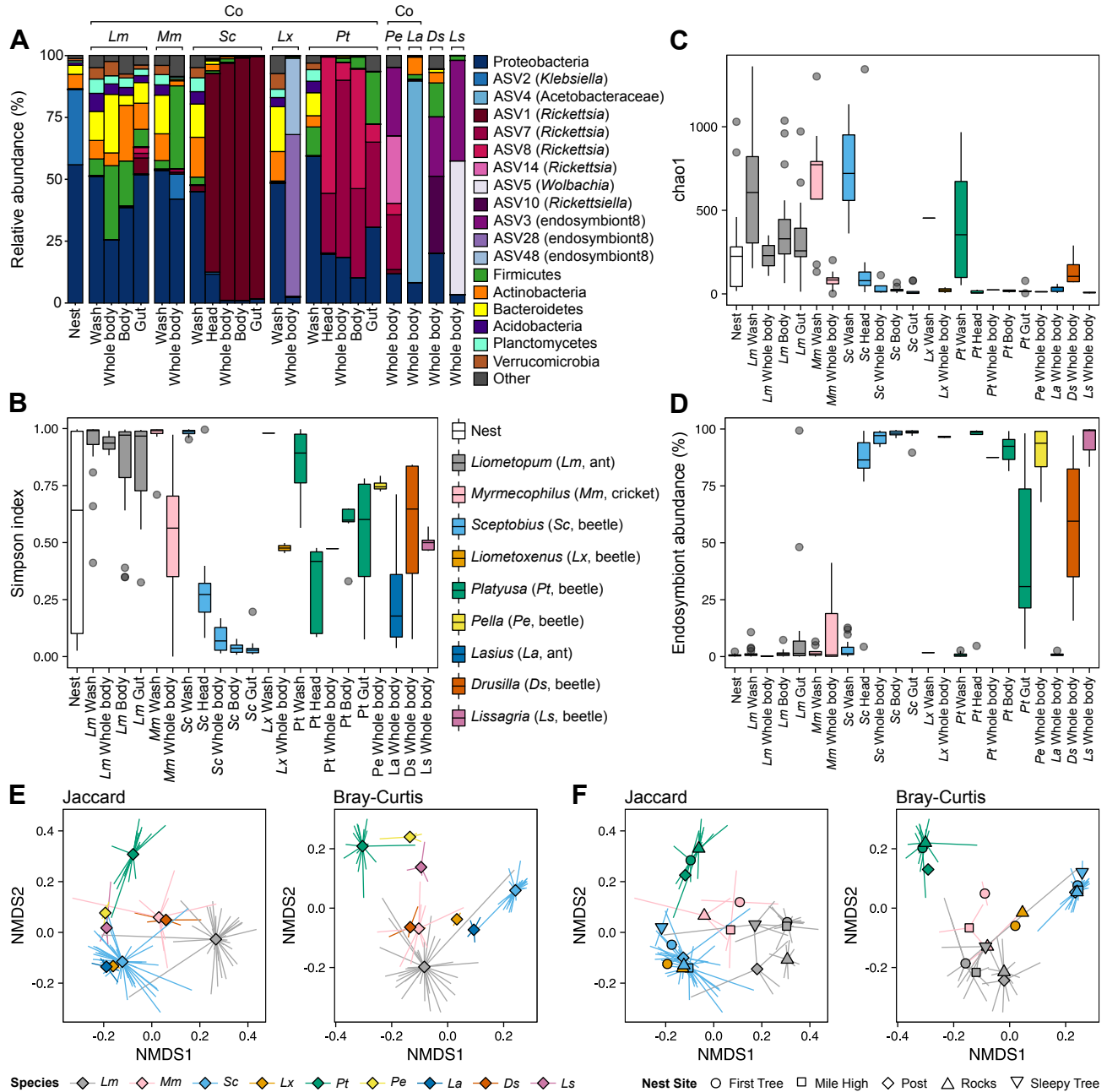
1221 **File S1.** Fasta file of contigs 1 and 2 of the genome of the *Rickettsia* endosymbiont of *Sceptobius*  
1222 *lativentris* (RiSlat).

1223 **File S2.** GenBank flat file with complete genome annotation of the *Rickettsia* endosymbiont of  
1224 *Sceptobius lativentris* (RiSlat).

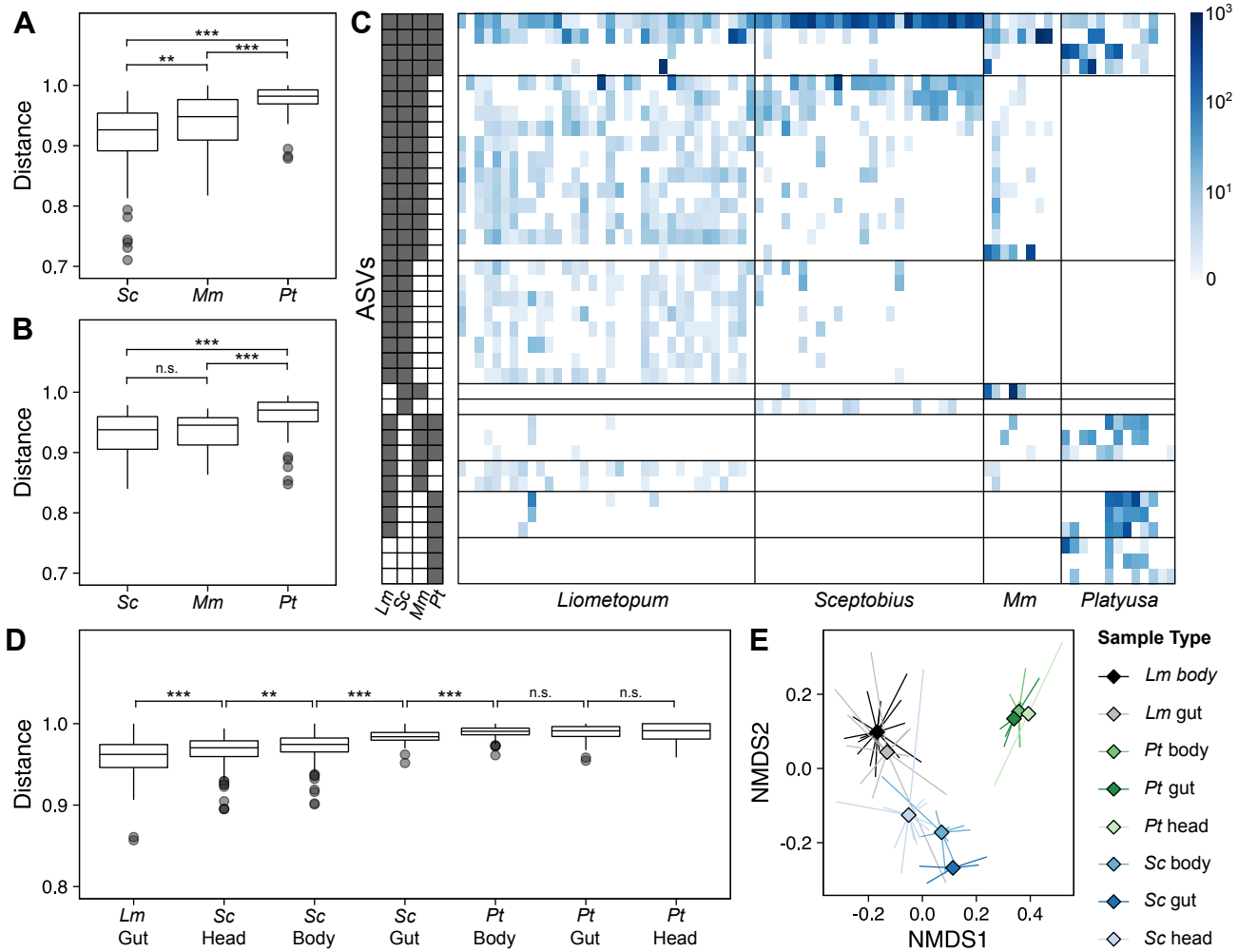


*Liometopum* core myrmecophile community

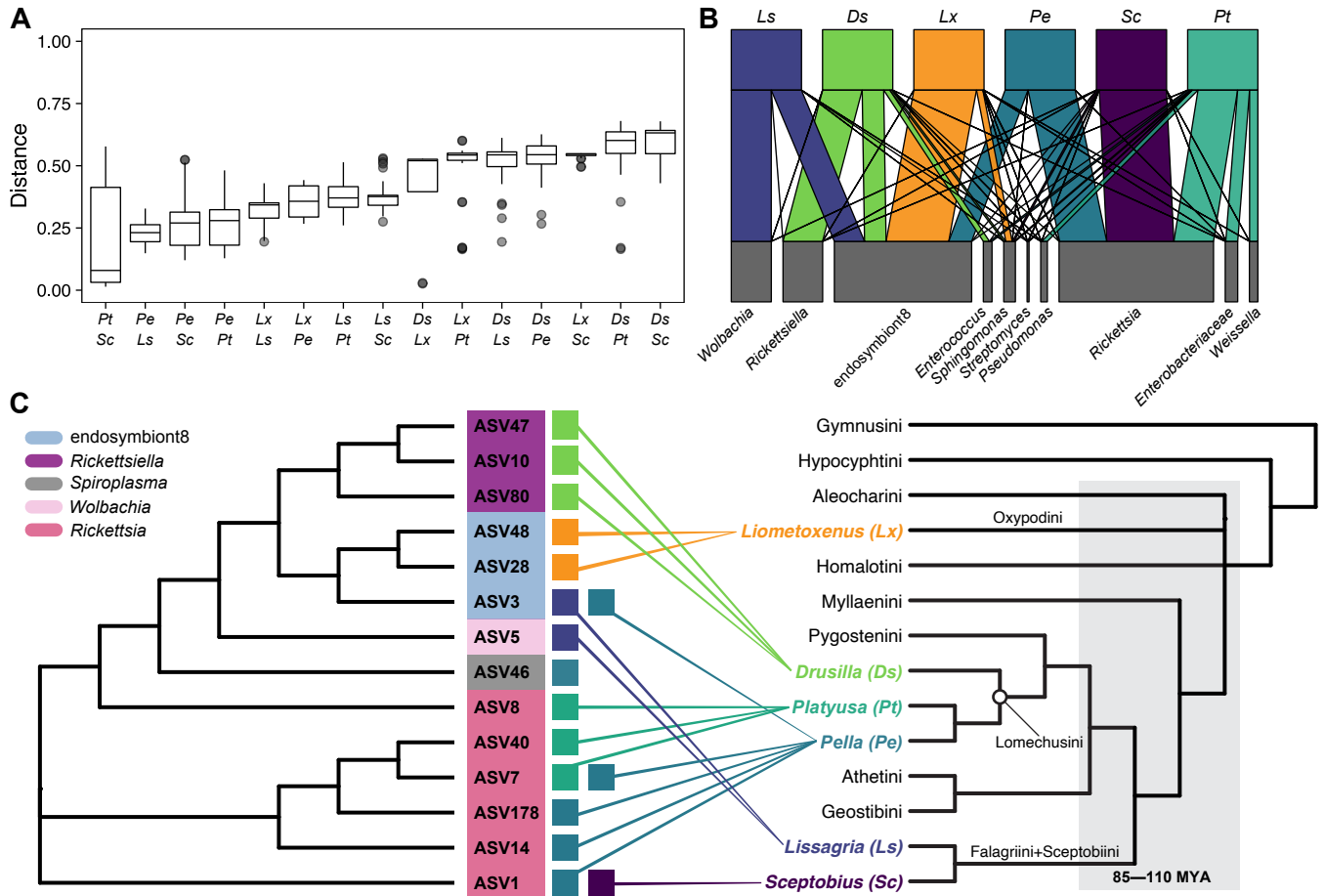




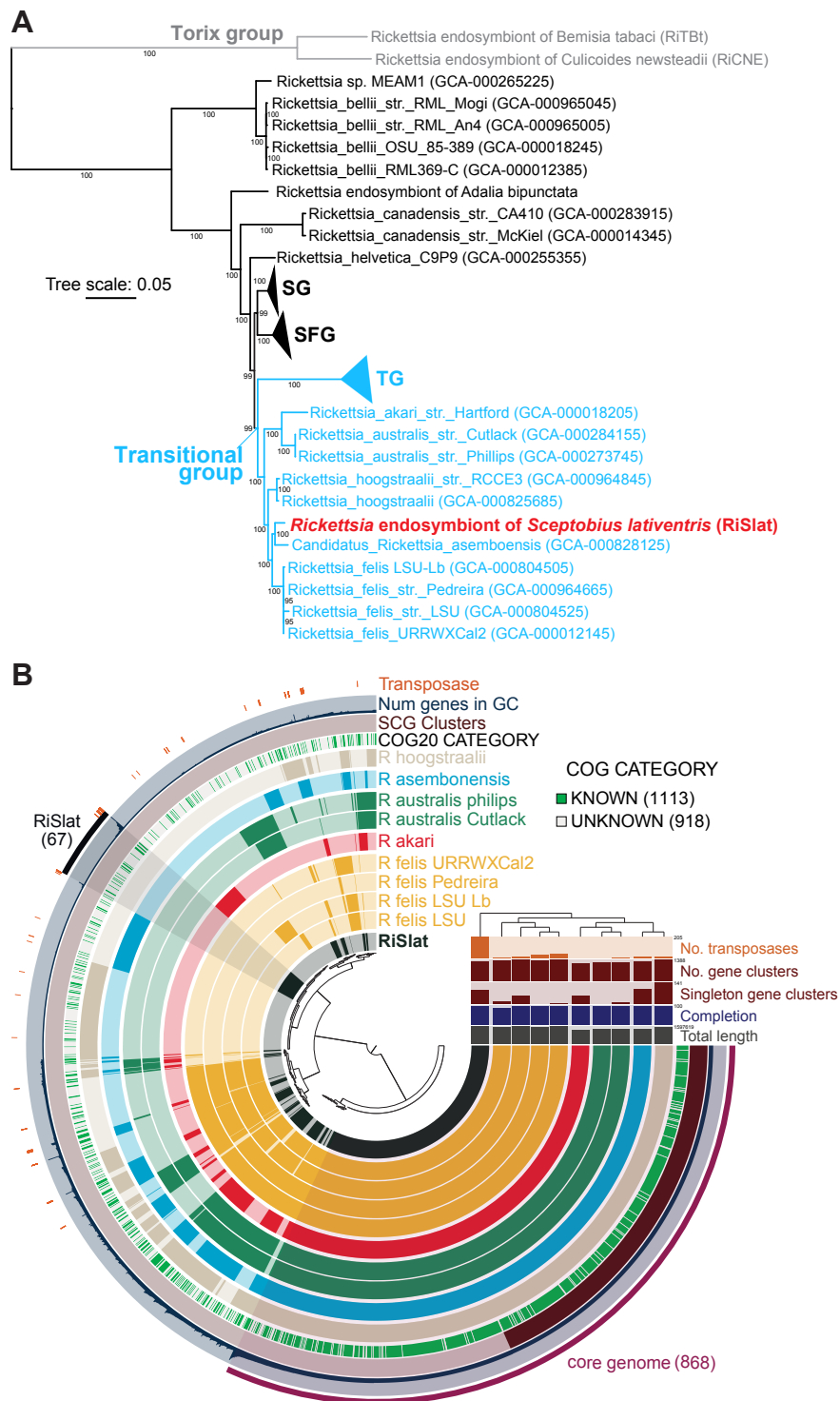
Perry et al Figure 2



Perry et al Figure 3

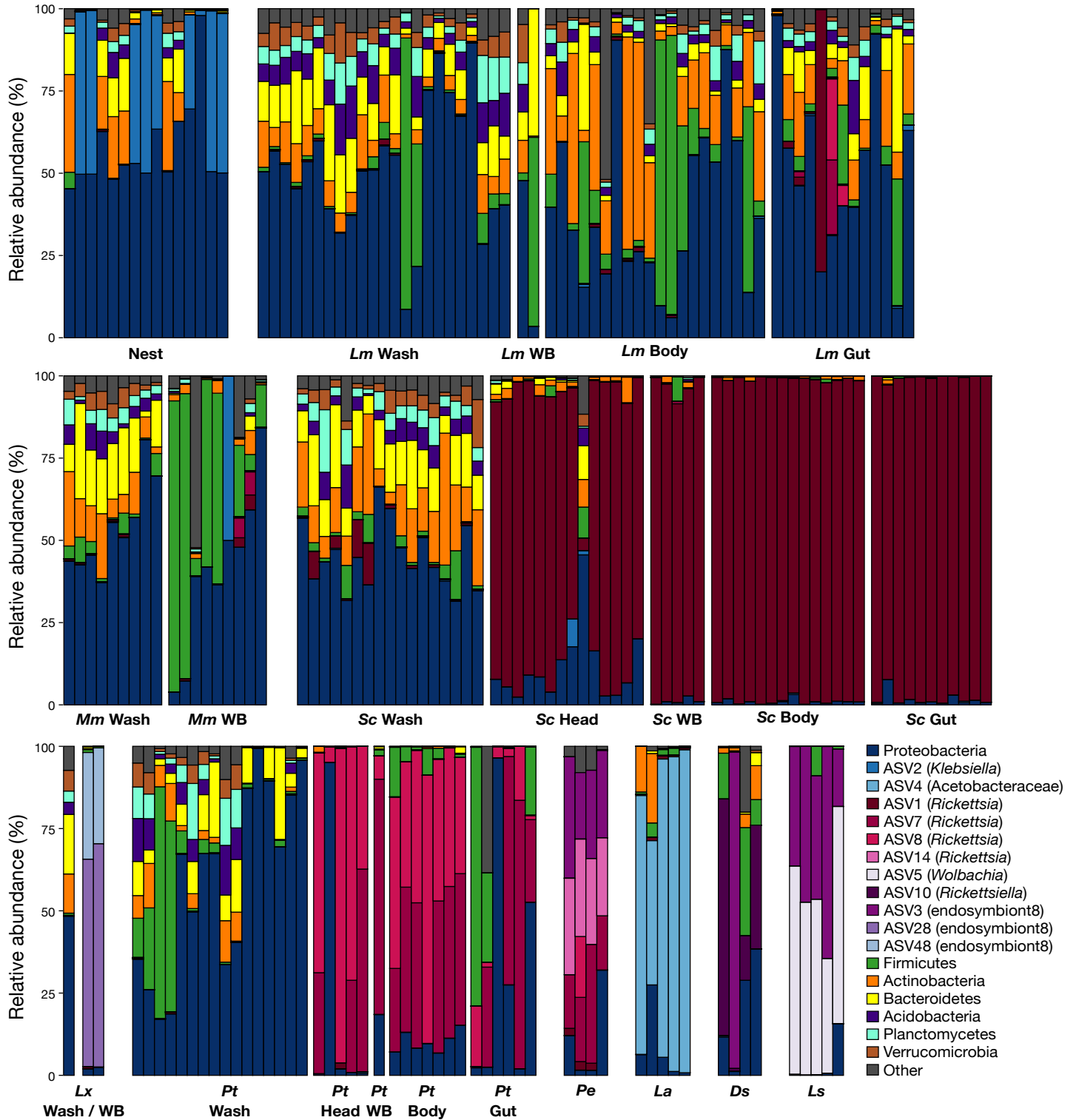


Perry et al Figure 4

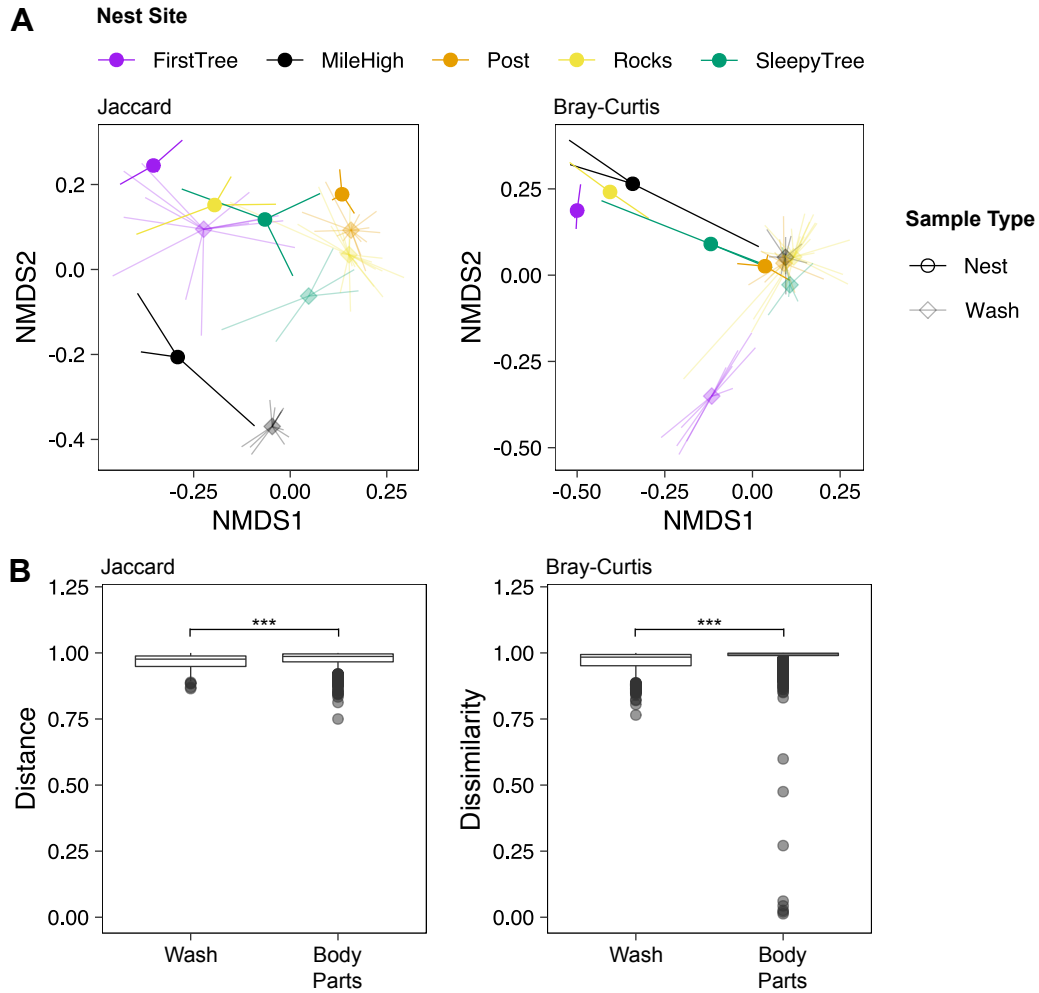


Perry et al Figure 5

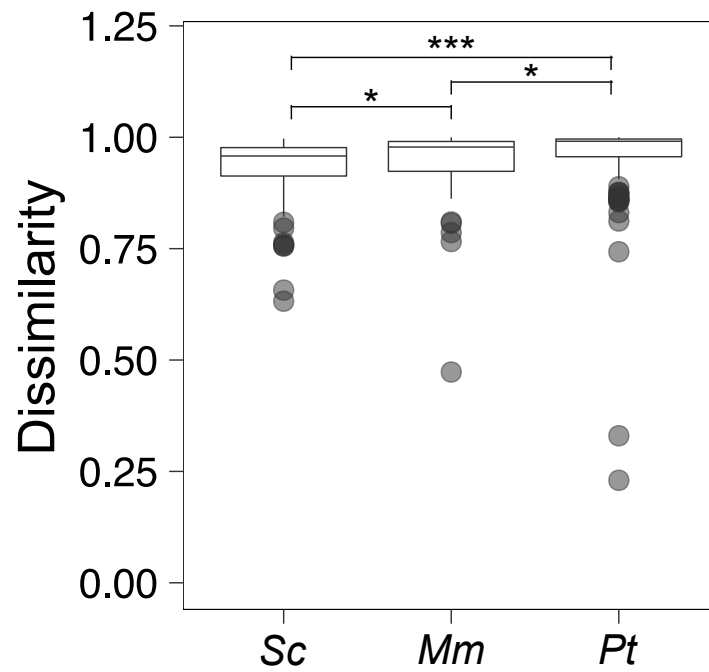




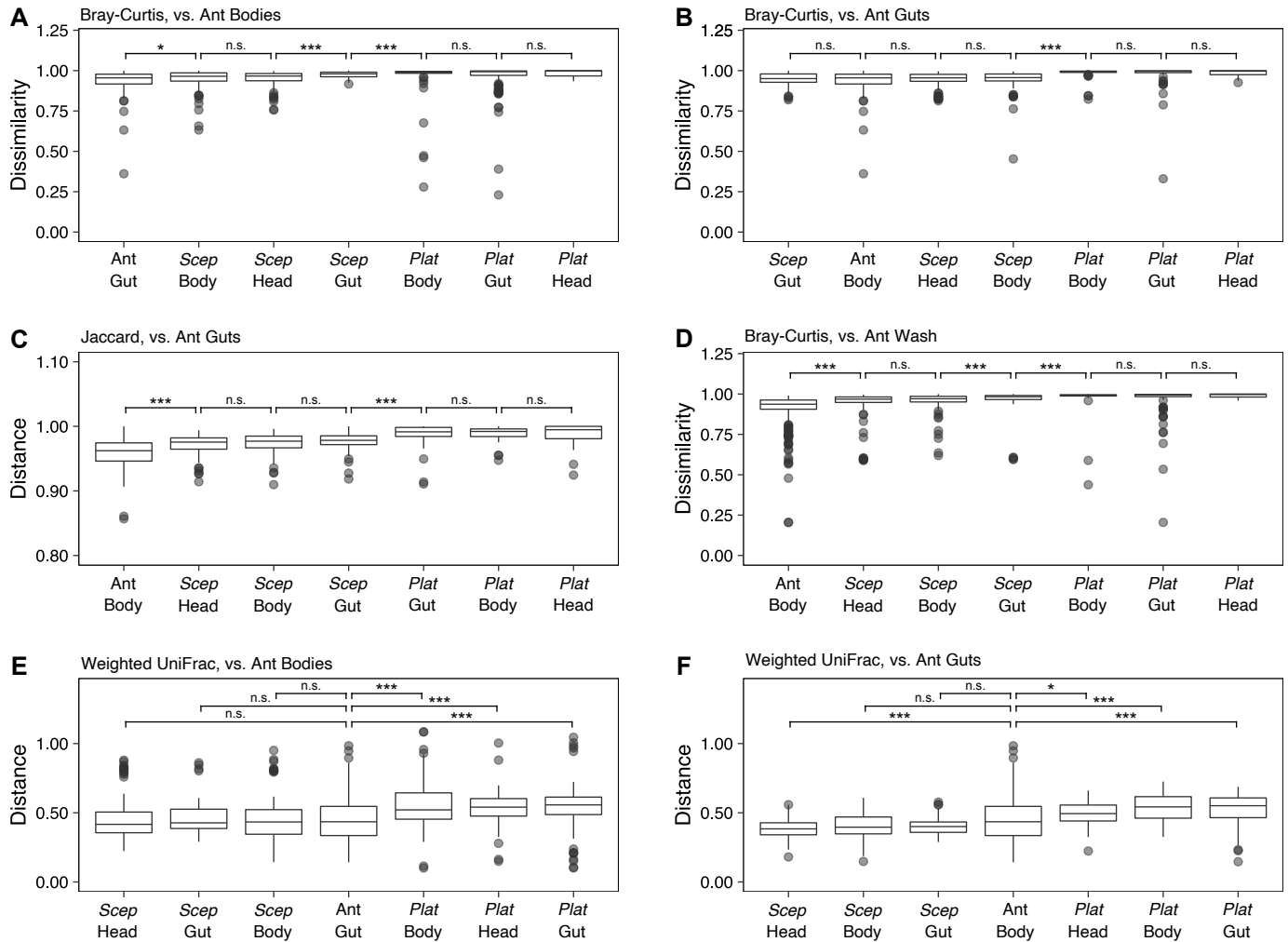
Perry et al Figure S1

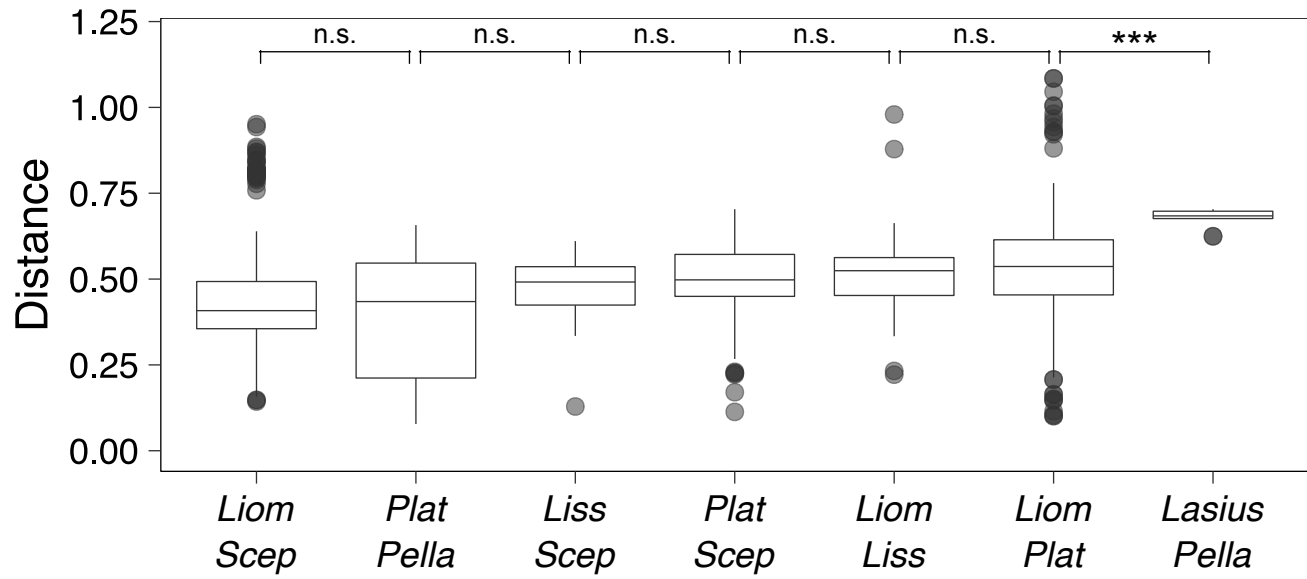


Perry et al Figure S2

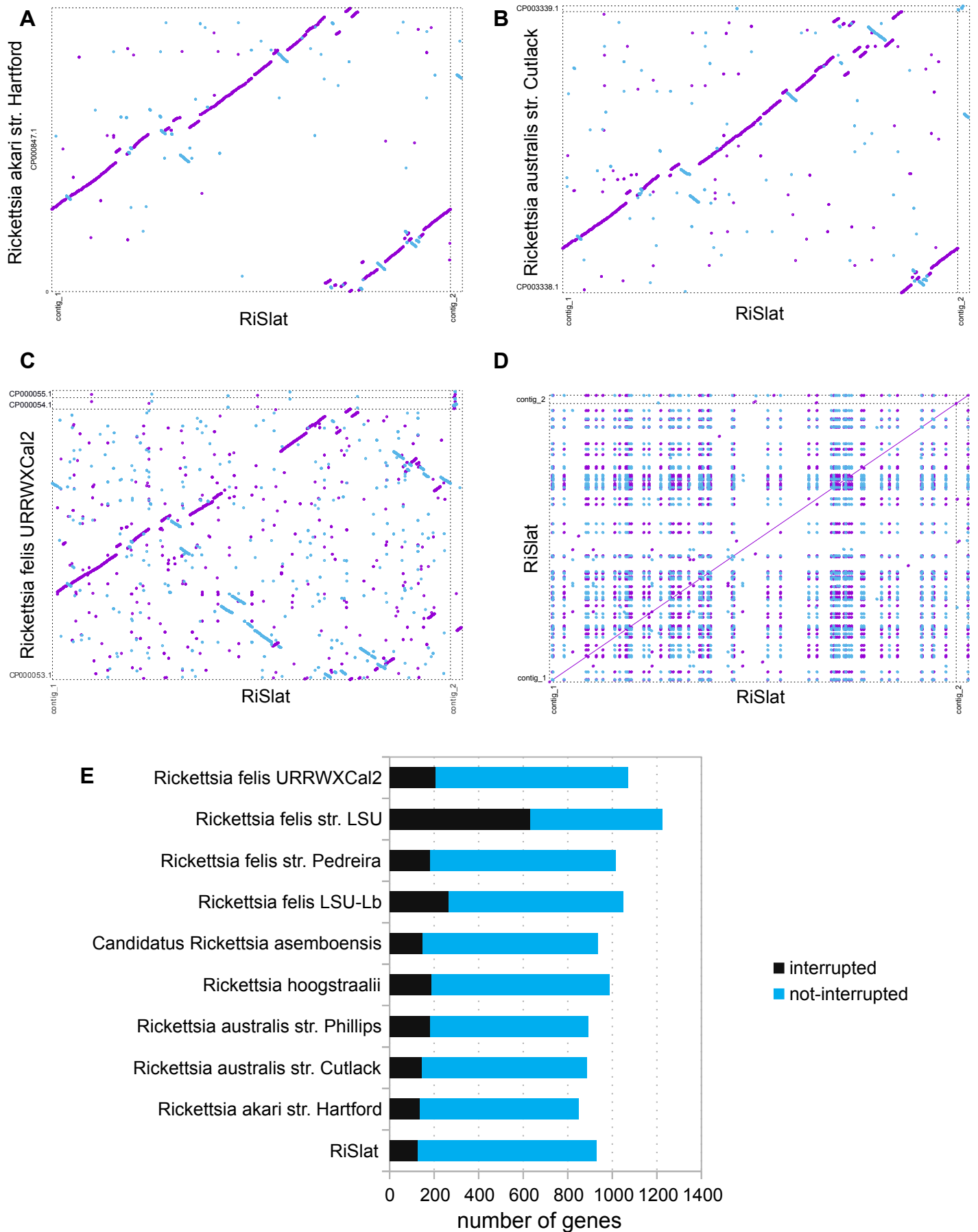


Perry et al Figure S3





Perry et al Figure S5



Perry et al Figure S6

